REMARKS

Reconsideration and reexamination of the subject application are respectfully requested in light of the foregoing amendments and following remarks.

1. Status of the Claims

The status of the claims following entry of the amendment is as follows:

Claims canceled: Claims 13-17 and 26-27

Claims pending: Claims 1-12 and 18-25

Claims allowed: None

Claims rejected: Claims 1-12 and 18-25

Claims withdrawn: None

2. Support for the Amendments

Claims 6 and 20 are amended solely to change the claims from which they depend.

3. Acknowledgement of Information Disclosure Statement

Applicants note with appreciation the acknowledgement of the Information Disclosure Statement filed August 5, 2008.

4. Rejections of the Claims Under 35 U.S.C. § 112, Second Paragraph

Claims 6 and 20 stand rejected under 35 U.S.C. § 112, second paragraph, as allegedly indefinite. The Office alleges that "the JCV agnoprotein" lacks antecedent basis. Claims 6 and 20 are amended to depend from claims 5 and 19, respectively, thereby providing proper antecedent basis. The rejection accordingly may be withdrawn.

5. Rejection of the Claims Under 35 U.S.C. § 112, First Paragraph

Claims 1-12 and 18-25 stand rejected under 35 U.S.C. § 112, first paragraph, as failing to comply with the enablement requirement. Applicants traverse the rejection.

The Office maintains the rejection on the basis that Applicants have not established whether *in vitro* efficacy, exemplified in the specification, correlates with *in vivo* efficacy, as claimed. The specification discloses *in vitro* efficacy in the U87MG cell line. *See, e.g.*, Specification, Example 1. In this example, a representative agnoprotein was introduced into U87MG cells in an amount effective to inhibit the growth of the cells, as claimed. *See, e.g.*, Specification, p. 30, lines 3-12, and p. 31, line 36, through p. 32, line 5. Further experiments showed the same result with NIH 3T3 cells. *See, e.g.*, Specification, p. 32, line 7, *et seq.*

Efficacy in a cell model or animal model constitutes a "working example" if that example "correlates" with a disclosed or claimed method invention. *See* Manual of Patent Examining Procedure (MPEP) § 2164.02, "Working Example," 8th ed., revised Aug. 2006 (relying on *In re Brana*, 51 F.3d 1560, 1566, 34 U.S.P.Q.2d 1436, 1441 (Fed. Cir. 1995). Only a reasonable correlation is required—not a rigorous or an invariable exact correlation. *See Cross v. Iizuka*, 753 F.2d 1040, 1050, 224 U.S.P.Q. 739, 747 (Fed. Cir. 1985).

In the present case, the Office and Applicants disagree whether the skilled artisan would have accepted successful tests for efficacy in the human U87MG cell line as correlating with a method of treating glioblastoma *in vivo*. The Office cites two references, Gura, *Science* 278: 1041-42 (1997) ("Gura") and Jain, *Scientific Am.* July: 58-65 (1994) ("Jain") to support its allegations. Gura purportedly teaches that screening in cell and animal models since 1955 has identified only 39 drugs that ultimately won approval from the Federal Food and Drug Administration (FDA). *See* Gura, p. 1041, 1st col. Jain purportedly teaches that encouraging laboratory results often are not predictive of success in treating solid tumors *in vivo*. *See* Jain, p. 65. The Office concludes that Gura and Jain are probative of the enablement, or lack thereof, of the claimed invention. *See* Office Action, p. 3, ¶ 2.

Gura and Jain may support the general proposition that biotechnology is a relatively unpredictable art, but this is only one of the many factors to be weighed in an analysis of enablement. *See In re Wands*, 858 F.2d 731, 737, 8 U.S.P.Q.2d 1400, 1404

(Fed. Cir. 1988). Gura and Jain, however, are irrelevant to whether the disclosed example in the specification constitutes a working example of the claimed invention, because clinical success is not required as proof of enablement. Rather, the FDA determines whether compounds are safe and effective in the treatment of humans, not the USPTO. *See In re Brana*, 34 U.S.P.Q.2d 1436, 1442 (Fed. Cir. 1995). Gura and Jain may suggest uncertainty regarding FDA approval for ***any*** method of treating cancer, but Gura and Jain have little bearing on the issue of whether the ***claimed invention*** is enabled. In particular, Gura and Jain have no bearing whatever on the issue of whether the disclosed tests with the U87MG cell line constitute a working example of the claimed invention.

While the Office does not explicitly require clinical tests as proof of enablement, the Office alleges that the exemplified *in vitro* results do not correlate with *in vivo* results on the basis of the failure of clinical studies disclosed in Gura and Jain. Office Action, p. 3, ¶ 2. It follows that the only way to show correlation, under the Office's test, is to provide evidence of successful clinical tests. A requirement for clinical trials to prove correlation is a *de facto* (improper) requirement for clinical trials to prove enablement. Respectfully, the Office errs by setting the test for correlation too high, i.e., far higher than the Federal Circuit's test. The Federal Circuit holds that only a reasonable correlation is required—not a rigorous or an invariable exact correlation. *See Cross*, 753 F.2d at 1050, 224 U.S.P.Q. at 747.

Applicants comply with the Federal Circuit's test, for the following reasons. The Federal Circuit holds that *in vitro* tests can provide sufficient evidence of enablement. *See Brana*, 34 U.S.P.Q.2d at 1440 ("If applicants were required to wait until an animal naturally developed this specific tumor before testing the effectiveness of a compound against the tumor *in vivo*, . . . there would be no effective way to test compounds *in vivo* on a large scale."); *see also Cross*, 224 U.S.P.Q. 747-48. Zhao *et al.*, *Int'l J. Oncol.* 21: 49-55 (2002) ("Zhao") and Yoshida *et al.*, *Neurosurgery* 39: 360-66 (1996) ("Yoshida") support a conclusion that the skilled artisan used U87MG cells expressly because the efficacy of a compound in this cell line indicated the potential usefulness of the compound for *in vivo* treatment. *See, e.g.*, Zhao, p. 49 ("The present evidence that As_2O_3

at relatively low concentration effectively inhibited proliferation of U87MG and T98G cells *in vitro*, suggests that the drug may be considered for *in vivo* testing on animal models and possibly clinical trials on glioma patients."); Yoshida, *2 ("This [*in vitro*] study was designed to determine whether the motility and invasiveness of glioblastoma cells could be influenced by treatment with [estramustine phosphate] and to correlate those findings with the ability of the agent to inhibit proliferation. Suppression of the infiltrative capacity of malignant glioma cells could be of significant value in the treatment of those lesions."). Zhao and Yoshida thus provide sufficient, relevant, and objective evidence that the skilled artisan expected successful tests for efficacy in the human U87MG glioblastoma cell line to correlate with a method of treating glioblastoma *in vivo*. It follows that the example in the specification using the U87MG glioblastoma cell line is a working example of the claimed invention, supporting a conclusion of enablement. *See Wands*, 858 F.2d at 737, 8 U.S.P.Q.2d at 1404.

The Office, however, discounts the evidence of enablement from Zhao and Yoshida. The Office particularly alleges that neither Zhao nor Yoshida teach whether drugs tested in cell models were later shown to inhibit cell growth *in vivo*. *See* Office Action, ¶ bridging pp. 3-4. Certainly, the ***skilled artisan*** expects successful testing in U87MG cells to lead to effective treatments *in vivo*. Like Zhao and Yoshida, Hoshi *et al.*, *Cancer Gene Ther.* 7: 799-805 (2000) ("Hoshi")[1] states that an effective U87MG cell-killing compound with demonstrated *in vitro* efficacy "is expected to be clinically useful for the treatment of malignant brain tumors." Hoshi, p. 804, 1st col., ¶ 6. Zhao, Yoshida, and Hoshi expect clinical success in view of success *in vitro*. It is the Office's burden to provide evidence to the contrary, which evidence is lacking in the present case. *See In re Marzocchi*, 439 F.2d 220, 224, 169 U.S.P.Q. 367, 370 (C.C.P.A. 1971).

Finally, the Office alleges that the present case is distinguished over *Brana* because there is no evidence in the present record that *in vitro* success using the U87MG cell line is recognized in the art as correlating specifically with *in vivo* efficacy. That is, there allegedly is no evidence that a drug used *in vitro* in U87MG cells later showed

[1] A copy of Hoshi is attached hereto as Exhibit 1.

efficacy *in vivo*. Eshleman *et al.*, *Cancer Res.* 62: 7291-97 (2002);[2] Seely *et al.*, *BMC Cancer* 2: 15 (2002);[3] Pinski *et al.*, *J. Clin. Endocrin. Metab.* 77: 1388-92 (1993);[4] and Blanquicett *et al.*, *Mol. Cancer Ther.* 1: 1139-45 (October 2002)[5] collectively support the conclusion that compounds showing efficacy in U87 cells *in vitro* also show efficacy when tested *in vivo*, e.g., in brain tumors formed by U87 xenografts in nude mice. For all the reasons above, Applicants have produced sufficient reasons and evidence to support a conclusion that the present invention is enabled. The rejection accordingly should be withdrawn.

2 A copy of Eshleman is attached hereto as Exhibit 2.
3 A copy of Seely is attached hereto as Exhibit 3.
4 A copy of Pinski is attached hereto as Exhibit 4.
5 A copy of Blanquicett is attached hereto as Exhibit 5.

CONCLUSION

In conclusion, this amendment and reply is believed to be a full response to the outstanding Office Action. Should any issues remain outstanding or if there are any questions concerning this paper, or the application in general, the Examiner is invited to telephone the undersigned representative at the Examiner's earliest convenience.

If there are any other fees due in connection with the filing of this response, please charge the fees to our Deposit Account No. 50-0573. If a fee is required for an extension of time under 37 C.F.R. § 1.136 not accounted for above, such an extension is respectfully requested and the fee should also be charged to our Deposit Account.

Respectfully submitted,

Date: January 5, 2009

By: Brian Pattison, Reg No. 43,740
for DANIEL A. MONACO
Registration No. 30,480
DRINKER BIDDLE & REATH LLP
One Logan Square
18th and Cherry Streets
Philadelphia, PA 19103-6996
(215) 988-3312 - Phone
(215) 988-2757 – Fax
Attorney for Applicant

Exhibit 1

Antitumoral effects of defective herpes simplex virus-mediated transfer of tissue inhibitor of metalloproteinases-2 gene in malignant glioma U87 *in vitro*: Consequences for anti-cancer gene therapy

Michio Hoshi,[1,2] Asako Harada,[1] Takeshi Kawase,[2] Keiichi Uyemura,[1] and Takahito Yazaki[1,2]

Departments of [1]Physiology and [2]Neurosurgery, School of Medicine, Keio University, Tokyo, Japan.

We set up experiments to evaluate the effects of defective herpes simplex virus (HSV)-mediated *in vitro* gene transfer of tissue inhibitor of metalloproteinases-2 (TIMP-2) in malignant glioma cells. Intrinsic TIMPs are known to be inhibitors of the strong invasive activities of matrix metalloproteinases in malignant gliomas. The defective HSV vectors dvSRaTIMP2 was engineered to express human TIMP-2 (hTIMP-2) with a combination of replication-competent HSV mutant, temperature-sensitive HSV-tsK, and amplicon plasmid-containing hTIMP-2. The *hTIMP-2* gene was driven by the *simian virus 40 promoter*. The helper virus (HSV-tsK) was thermosensitive; consequently, this vector could proliferate only at 31.5°C. After infection of U87 human glioblastoma cells with the vector *in vitro*, expression of TIMP-2 was confirmed by reverse zymography. The U87 cells infected *in vitro* either with dvSRaTIMP2 or HSV-tsK were efficiently destroyed under replication-permissive conditions (at 31.5°C) and significantly lowered under replication-nonpermissive conditions (at 37°C). The invasive activity of U87 was clearly inhibited by dvSRaTIMP2 infection at both 31.5°C and 37°C. Our studies suggest that TIMP-2 expressing the defective HSV vector is possibly useful for the treatment of malignant brain tumors. **Cancer Gene Therapy (2000) 7, 799–805**

Key words: Gene therapy; glioma; herpes simplex virus type-1; matrix metalloproteinase; tissue inhibitor of metalloproteinases.

Gliomas are the most common primary human brain tumors. The prognoses of patients with malignant astrocytoma and glioblastoma multiforme are the poorest of all of the brain tumors, although these tumors rarely metastasize systemically. Because most gliomas, especially glioblastomas, aggressively invade and spread into normal brain parenchyma, from which the margins of the tumor are undistinguishable, it is almost impossible to totally remove these tumors. Because control of these tumors is difficult, local tumors often demonstrate recurrence after initial treatment. This recurrence may contribute to an extremely poor prognosis for patients with malignant glial tumors. Recently, human gene therapy has shown great potential as a therapeutic method for these malignant tumors.

Previous studies have demonstrated that herpes simplex virus-1 (HSV-1) mutants are effective not only for the killing of malignant brain tumors[1,2] but also for the transfer of a foreign gene to target cells and for ensuring adequate expression of the transferred gene *via* defective particles.[3–5] We have tried to develop a more efficient strategy with a replication-competent HSV helper/defective viral system that expresses proteinase inhibitors, resulting in both cytotoxicity and inhibition of invasion.

Invasive tumors are known to produce extracellular matrix-degrading enzymes, such as matrix metalloproteinases (MMPs),[6–11] heparinases, plasminogen activators, cathepsins,[12] and brain-enriched hyaluronan binding/brevican.[13] The MMP family, especially MMP-2 (72-kDa gelatinase/type IV collagenase/gelatinase A), plays a key role in invasive activity.[6–8] Tissue inhibitors of metalloproteinases (TIMPs) are secreted by tumor cells and block the activities of MMPs.[8,10,14–16]

In the present study, we demonstrate that human TIMP-2 (hTIMP-2) expression *via* defective particles inhibits tumor invasion efficiently for the U87 cell line, synchronously with the cytotoxic action of HSV-tsK, which replicates at 31.5°C *in vitro*.

Received June 24, 1999; accepted November 24, 1999.

Address correspondence and reprint requests to Dr. Takahito Yazaki, Department of Physiology, School of Medicine, Keio University, Tokyo 160-8582, Japan. E-mail address: yazakit@med.keio.ac.jp

MATERIALS AND METHODS

Cell lines

Human glioma cell lines (U87, SW1088, and U251) and Vero (African green monkey kidney) cells were obtained from the American Type Culture Collection (Manassas, Va). These cells were maintained in Dulbecco's modified Eagle's medium

(DMEM) (Nissui Pharmaceuticals, Tokyo, Japan) with 10% heat-inactivated fetal bovine serum and antibiotics (Sigma, St. Louis, Mo) at 37°C. Passages were usually performed twice a week with 0.25% trypsin-ethylenediaminetetraacetic acid solution (Sigma).

pSRaTIMP2 amplicon plasmid construction

A plasmid containing *hTIMP-2 cDNA* cloned between the *Eco*RI and the *Bam*HI sites of pSG5 (Stratagene, La Jolla, Calif) was provided by Dr. Seiki (Department of Cancer Cell Research, Institute of Medical Science, University of Tokyo, Tokyo, Japan). pSRaTIMP2 was constructed by inserting a *Sal*I fragment from this plasmid, which has a *simian virus 40 promoter* upstream and a *poly(A)* sequence downstream, at the restriction site for *Sal*I of pSRa-ori4 amplicon vector, which was provided by Dr. Samuel D. Rabkin (Department of Neurosurgery, Georgetown University Medical Center, Washington, DC).

Generation of dvSRaTIMP2, hTIMP-2-expressing HSV-1 helper/defective virus vector

pSRaTIMP2 amplicon plasmid was transfected into Vero cells using Lipofectamine Plus reagent (Life Technologies, Gaithersburg, Md). After incubation overnight at 37°C, the medium was removed; the cells were superinfected with the HSV-tsK strain (provided by Dr. Subak-Sharpe, Institute of Virology, Glasgow, UK) at a multiplicity of infection (MOI) of 0.2 and cultured at 31.5°C in DMEM with 1% fetal bovine serum. Viral stocks were generated according to the method described by Kaplitt et al.[17] Titration of HSV-tsK helper virus in the viral stocks was determined by a plaque-forming assay at 31.5°C; titration of the defective particles was assayed *via* immunohistochemical detection of hTIMP-2. hTIMP-2 antibody was obtained from Fuji Chemical Industries (Takaoka, Japan). The primary antibody was visualized by the avidin-biotin complex technique (Vector Laboratories, Burlingame, Calif) with diaminobenzidine tetrahydrochloride. The MOI of helper virus was shown to be that of dvSRaTIMP2. The best stock appeared at passage 5. The titer of the best stock was 3.2×10^8 plaque-forming units/mL (helper virus) and 3.3×10^6 defective particle units/mL (defective particles), with a defective/helper ratio of 1.0×10^{-2}.

Cell culture cytotoxicity

To determine the *in vitro* cytopathic efficacy of HSV-tsK and dvSRaTIMP2, ~1×10^4 cells in 1 mL of DMEM with 10% fetal calf serum (FCS) were seeded in a 12-well plate; on the following day, the number of cells was counted in the same manner as on day 0. HSV-tsK or dvSRaTIMP2 was applied to the cells at MOIs of 0.1, 0.5, and 1.0 and cells were cultured at 31.5°C and 37°C. The numbers of viable cells were determined by the trypan blue (Life Technologies, Grand Island, NY) exclusion method on days 1–5. All experiments were performed in triplicate.

Gelatin zymography

Gelatin zymography was performed according to previous reports with modifications.[7,10,18] Briefly, the samples were subjected to a 10% sodium dodecyl sulfate polyacrylamide gel containing 0.1% gelatin (Sigma). After electrophoresis at 4°C, gels were washed in 2.5% Triton X-100 at 4°C for 1 hour and incubated in incubation buffer (50 mM tris(hydroxymethyl) aminomethane (pH 7.5), 10 mM $CaCl_2$, 1 μM $ZnCl_2$, 0.02% NaN_3, and 1 mM phenylmethylsulfonyl fluoride) at 37°C for 20 hours. The gels were then stained with 0.1% Coomassie brilliant blue R-250 (Nacalai Tesque, Kyoto, Japan) and destained in a solution of 10% acetic acid and 50% methanol. The proteolytic activities of the gelatinases were detected as unstained bands.

MMP-2 activities

Cells (1×10^5 cells) were placed in 500 μL of serum-free DMEM/24-well plates and incubated for 24 hours. Serum-free conditioned medium was centrifuged, and the supernatant was used for gelatin zymography as described above. Each sample was mixed with the same volume of 2× sample buffer without reducing agents, and 10 μL of each sample was used for gelatin zymography. Samples were not heated before electrophoresis. The gels were scanned after destaining, and a quantity of MMP-2 was obtained by determination of the lytic zone areas with Adobe PhotoShop (Adobe Systems, San Jose, Calif). The intensity of negative staining is linear in the range of 25–500 μU per lane, which was used for quantity for MMP-2 activities.

To determine the difference between the MMP-2 activities at 31.5°C and 37°C, 2 μL, 4 μL, and 8 μL of U87-conditioned media with 2× sample buffer without reducing agents were subjected to electrophoresis at 4°C. Each sample was duplicated on the same gel. After electrophoresis, the gels were treated with Triton X-100 as described above. The gels were then separated, and each gel was immersed in incubation buffer at 31.5°C and 37°C. The intensity of the negative staining bands was measured as described above.

Reverse zymography

The TIMP-2 secreted into the culture medium was detected with reverse zymography. Cells (8×10^5) in 2 mL of serum-free DMEM were cultured in a 6-well plate with or without viruses at various MOIs for 3 days. Each conditioned medium was centrifuged, and each 20 μL of supernatant and 4× sample buffer was used for reverse zymography as follows.

Reverse zymography was performed according to a procedure described previously with modifications.[6,14] Briefly, the samples and recombinant hTIMP-2 (Fuji Chemical Industries) were subjected to a sodium dodecyl sulfate-15% polyacrylamide gel containing 0.3% gelatin. After electrophoresis at 4°C, gels were incubated in 2.5% Triton X-100 at 4°C for 1 hour and incubated in incubation buffer at 37°C for 20 hours. Next, the gels were destained as described above. With this technique, the dark zones appearing on the gel indicated the presence of gelatinase inhibitors.

Transwell chamber assay

To determine the effects of HSV-tsK- and hTIMP-2-expressing defective virus (dvSRaTIMP2) on U87 cells, we used an *in vitro* invasion assay system.[6,10] Six-well transwell chambers (Bio-Coat; Becton Dickinson Labware, Bedford, Mass) with 8-μm pores were coated with Matrigel (100 μg/cm^2; Becton Dickinson Labware) and allowed to air-dry overnight. The Matrigel was reconstituted with 2 mL of serum-free DMEM at room temperature for 2 hours.

Following the manufacturer's guidelines, 2 mL of cell suspension (8×10^5 cells) in serum-free DMEM was added into triplicate upper chamber wells. HSV-tsK or dvSRaTIMP2 was then infected at an MOI of 0.1 at 31.5°C and at an MOI of 1.0 at 37°C.

After 72 hours of incubation at 31.5°C or 37°C, the number of cells attached to the lower well having traversed the filter

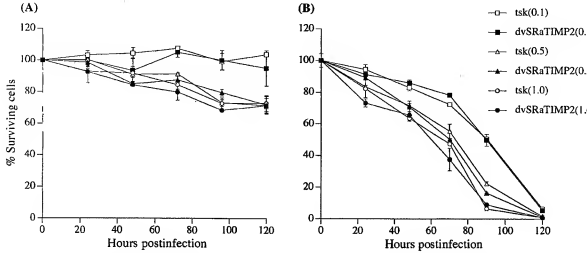

Figure 1. Effects of tsK and dvSRaTIMP2 on U87 malignant gliomas *in vitro*. U87 cell cultures were infected with tsK or dvSRaTIMP2 at MOIs of 0.1, 0.5, and 1.0. **A:** Cells cultured at 37°C. **B:** Cells cultured at 31.5°C. Numbers in parentheses indicate MOIs. Data are mean ± SE.

was counted in 10 random fields at ×100 magnification. The percentage of invasion was determined by the ratio of the number of cells infected by each virus invading through the Matrigel insert membrane to the mean number of cells without viral infection migrating through the control insert membrane without Matrigel at the same temperature.

Statistical analysis

Results were expressed as the mean ± SE. Statistical analyses were performed with Student's *t* test. Statistical significance was set at the 5% level ($P < .05$).

RESULTS

In vitro *cytopathic efficacy*

U87 cells showed approximately a 2.5-fold higher growth rate when cultured at 37°C than at 31.5°C. The doubling time was 33.3 hours at 37°C and 84.1 hours at 31.5°C.[7] At 72 hours postinfection, the percentage of surviving U87 cells at 37°C infected with HSV-tsK and dvSRaTIMP2 at an MOI of 1.0 was 84.5 ± 2.9 and 79.8 ± 5.1% (mean ± SE), respectively (Fig 1A), whereas the percentage of surviving U87 cells at 31.5°C infected with HSV-tsK and dvSRaTIMP2 at an MOI of 0.1 was 72.3 ± 0.2 and 78.1 ± 1.4%, respectively (Fig 1B).

The method of viral infection has been changed in the study of transwell chamber assay to estimate exact invasion ability. The methodological difference of viral infection between the usual plaque-forming assay and the transwell chamber assay is as follows. Briefly, in the plaque-forming assay, Vero cells were incubated with virus inoculum diluted in 1% FCS/phosphate-buffered saline at 37°C for 60 minutes; after aspiration of virus, cells were incubated with 1% FCS/DMEM at 31.5°C. In the transwell chamber assay, cells were infected by only applying virus to medium. Comparing the efficiency of infection between these methods, the number of cells infected by applying virus to medium was approximately one-third of that infected by plaque-forming assay (data not shown). Viral infection in the cytopathic assay was performed according to the same procedure as the

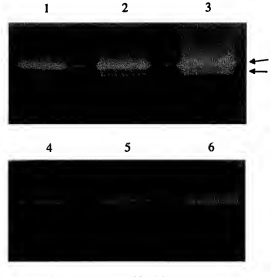

Figure 2. Zymography of MMP-2 in U87-conditioned medium. To compare the MMP-2 activities at 37°C with those at 31.5°C, zymography was performed. A total of 2 μL (lanes 1 and 4), 4 μL (lanes 2 and 5), and 8 μL (lanes 3 and 6) of U87-conditioned medium with 2× sample buffer without reducing agents was subjected to electrophoresis. After treatment with Triton X-100, gels were immersed in incubation buffer at 37°C **(top)** and 31.5°C **(bottom)** for 20 hours. The intensity of negative staining was linear in each of the three lanes. The ratio of the total MMP-2 activity incubated at 37°C to that at 31.5°C was 1.77 ± 0.05 (mean ± SE).

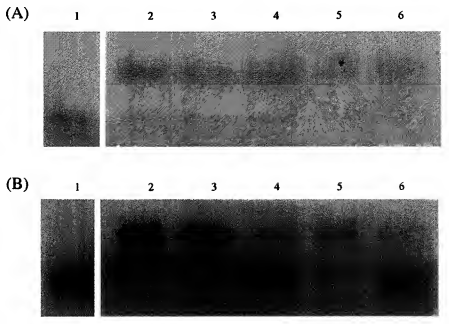

Figure 3. Reverse zymography of the media in which U87 cells were cultured without infection and with infection by viruses at various MOIs. After a 3-day culture at 37°C or 31.5°C, 20 μL of conditioned medium with sample buffer was used for reverse zymography. **A:** U87 cells cultured at 37°C. Lane 1, 5 ng of rTIMP-2; lane 2, no infection; lane 3, HSV-tsK infection (MOI of 0.2); lane 4, dvSRaTIMP2 infection (MOI of 0.2); lane 5, HSV-tsK infection (MOI of 1.0); lane 6, dvSRaTIMP2 infection (MOI of 1.0). hTIMP-2 expression by U87 cells without viral infection (lane 2) and with HSV-tsK infection at MOIs of 0.2 (lane 3) and 1.0 (lane 5) at 37°C was barely detectable. Cells infected with dvSRaTIMP2 (lanes 4 and 6), however, showed a greater expression of hTIMP-2. **B:** U87 cells cultured at 31.5°C. Lane 1, 5 ng of rTIMP-2; lane 2, no infection; lane 3, HSV-tsK infection (MOI of 0.2); lane 4, dvSRaTIMP2 infection (MOI of 0.2); lane 5, HSV-tsK infection (MOI of 0.5); lane 6, dvSRaTIMP2 infection (MOI of 0.5). It was obvious that the difference between the hTIMP-2 produced by dvSRaTIMP2-infected cells (lanes 4 and 6) and the hTIMP-2 produced by HSV-tsK-infected cells (lanes 3 and 5) appeared to be larger at 31.5°C than at 37°C.

transwell chamber assay. This fact should be taken into consideration.

MMP-2 activity and expression of hTIMP-2

The MMP-2 activities at 37°C of U87, SW1088, and U251 cells were 3.56 ± 0.22, 2.31 ± 0.20, and 0.98 ± 0.04 μU/cell (mean ± SE), respectively. The ratio of the total activity of MMP-2 of U87 cells reacted at 37°C to that at 31.5°C was 1.77 ± 0.05 μU/cell (mean ± SE; Fig 2).

By reverse zymography, the TIMP-2 activity was barely detectable both in the control and in HSV-tsK-infected U87 cells (MOIs of 0.2 and 1.0) at 37°C (Fig 3A, lanes 2, 3, and 5). However, by dvSRaTIMP2 infection at an MOI of 1.0, the cells showed a significantly higher expression of hTIMP-2 (Fig 3A, lane 6), whereas the expression of TIMP-2 by dvSRaTIMP2 at an MOI of 0.2 was similar to that seen for the samples infected with HSV-tsK (Fig 3A, lane 4). The difference between hTIMP-2 production in dvSRaTIMP2-infected cells and hTIMP-2 production in HSV-tsK-infected cells at 31.5°C was clearly larger than at 37°C (Fig 3B). A higher expression of hTIMP-2 was observed by reverse zymography with a higher titer of dvSRaTIMP2 infection.

Transwell chamber assay

The percentage of invasion of cells without any viral infection, with HSV-tsK infection, and with dvSRaTIMP2 infection through Matrigel membrane at 37°C was 10.2 ± 1.0, 9.1 ± 0.7, and 4.5 ± 0.8% (mean ± SE), respectively (Fig 4A). Although the invasive activity of HSV-tsK-infected cells was similar to the control (P = .35) at 37°C, the dvSRaTIMP2-infected cells clearly showed a lower invasive activity compared with the others ($P < .0001$). At 31.5°C, the percentage of invasion of cells with both viral infections (i.e., 3.4 ± 0.5% with HSV-tsK and 2.6 ± 0.3% with dvSRaTIMP2) was significantly different from the control (6.9 ± 0.7%; Fig 4B; $P < .0001$). There was some difference between the groups infected with HSV-tsK and those infected with dvSRaTIMP2, but this difference was not significant (P = .17).

DISCUSSION

In the present study, we demonstrated that the TIMP-2-expressing HSV-1 helper/defective virus vector dvSRa-TIMP2 has both a cytotoxic effect from the replication-competent helper virus and an invasive inhibitory effect due to secreted hTIMP-2 in the treatment of a malignant glioma cell line *in vitro*. The inhibition was clearly demonstrated by an invasion assay with the Matrigel basement membrane method.

Replication-defective HSV vectors have been widely used as gene-transfer vehicles into the central nervous

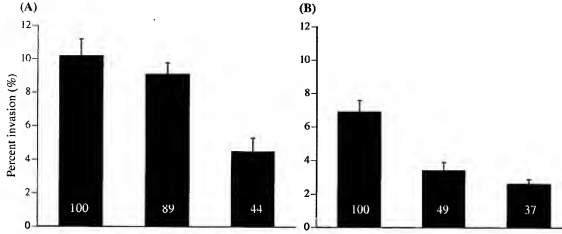

Figure 4. Effects of HSV-tsK and dvSRaTIMP2 on Matrigel assay of U87 cells. Cells were cultured at 37°C **(A)** and at 31.5°C **(B). A:** No significant difference was found between control and cells infected with tsK at 37°C ($P = .35$), but the difference between HSV-tsK and dvSRaTIMP2 was significant ($P < .0001$). **B:** A significant difference was detected between the control group and the other groups because of the cytotoxicity of HSV-tsK at 31.5°C. dvSRaTIMP2 had a tendency to decrease the number of cells traversing through Matrigel compared with HSV-tsK-infected cells, but the difference was not significant ($P = .17$). The numbers contained in the black bars are invasion indices when the percentage of invasion of control was set at 100% (mean ± SE).

system. The expression of immediate early genes from the helper virus may produce some toxicity in certain cell types, particularly at higher MOIs.[19] We remarked that the toxicity is useful to kill malignant tumor cells specifically, and we subsequently combined the replication-competent HSV-1 mutant with TIMP-2-expressing defective particles as an HSV-1 helper/defective virus vector.

Previous studies demonstrated that glioma cells express MMPs (especially MMP-2) that degrade the extracellular matrix and promote invasion.[6–9,16] The malignancy of the glioma was proportional to the gelatinase A mRNA expression.[15] The total activities of MMP-2 in the culture media of human glioma cell lines were quantified easily by gelatin zymography.

The activity of the MMP-2 secreted from U87 cells at 37°C was approximately twice that seen at 31.5°C (Fig 2), probably resulting in active invasion without viral infection at 37°C. Temperature-sensitive HSV-tsK is able to replicate and produce cell lysis at 31.5°C but not at 37°C.[20,21] This is why the percentage of invasion of U87 cells infected with HSV-tsK remarkably decreased at 31.5°C (invasion index = 50.0%) compared with that at 37°C (invasion index = 89.1%), even with an MOI that was 10 times higher. From the cell survival curve, HSV-tsK demonstrated very low cytotoxicity at 37°C (Fig 1).

According to Matrigel assay at 37°C, dvSRaTIMP2 infection remarkably inhibited the invasive activity of U87, whereas HSV-tsK did not show any significant inhibition. It was suggested that a large enough amount of hTIMP-2 was produced by defective viral particles at the high MOI to inhibit invasion, whereas only slightly higher activity was observed at 37°C by reverse zymography (Fig 3A). Although hTIMP-2 secretion at 31.5°C increased clearly from the dvSRaTIMP2-infected U87 cells, the percentage of invasion by dvSRaTIMP2-infected cells was not significantly decreased. At 31.5°C, the number of surviving cells decreased to 60–70% due to the cytotoxic effect of the helper particles (Fig 1B). Therefore, we probably could not detect significant inhibition of invasion despite the high TIMP-2 expression under this condition. Nakagawa et al[10] have shown that the invasive activity of another human glioma cell line (T98G) was inhibited with recombinant TIMP-2 (rTIMP-2), but not rTIMP-1 in a dose-dependent manner.

By infection with dvSRaTIMP2, the percentage of invasion decreased clearly in the Matrigel transwell chamber assay. As shown in Figure 1, the number of surviving cells after infection with dvSRaTIMP2 was similar to that seen after infection with HSV-tsK. This result supported a previous report indicating that addition of rTIMP-2 to the medium had no effect on glioma cell growth.[10] Collectively, the inhibition of invasion by dvSRaTIMP2 infection resulted from the inhibitory activity of hTIMP-2 to MMP-2, but not cell growth inhibition.

We demonstrated that dvSRaTIMP2 under replication-permissive conditions had a more potent ability to

inhibit U87 invasion than under replication-nonpermissive conditions. However, several tasks still remain to be completed.

First, temperature-sensitive HSV-tsK is barely able to replicate at normal human body temperature, but it can replicate at 31.5°C. Considering the experiments *in vivo*, it is therefore necessary to use an HSV that can replicate at 37°C.

Second, because the ratio of defective particle to helper virus in the viral stocks used in this study was low, a significant difference in the percentage of invasion was not seen between the tsK-infected group and the dvSRaTIMP2-infected group at 31.5°C. It is important to generate stocks with a higher ratio of defective particles because HSV infection at higher MOIs may reveal more cytotoxicity to normal cells as a result of its IE genes.[19]

Third, to reduce the activity of cell lysis by certain HSV-1 mutants themselves, it is useful to use HSV mutants that can replicate only in tumor cells and not in normal cells. An attenuated, multimutated HSV-G207[1] that is replication-competent in glioblastoma cells and other dividing cells provides additional safety features such as attenuated neurovirulence, temperature sensitivity and ganciclovir hypersensitivity, and the presence of an easily detectable histochemical marker, the *lacZ* gene. HSV-G207 was also effective for the treatment of intracranial malignant meningiomas without inflammation, hemorrhage, or other pathological effects in the surrounding normal brain tissue.[2] HSV-G207 might be used as a helper virus in this study.

Fourth, most people of >40 years of age are presumed to be infected with HSV-1. In the presence of wild-type HSV-1 and HSV-1 antibody, we should consider two possibilities regarding gene therapy *via* HSV. First, the revertants arise frequently (10^{-5}-10^{-6}) and are related to the extent of overlapping homology between the integrated gene and the wild-type gene.[22–24] The application of multimutated HSV, rather than single-mutated HSV, can decrease it remarkably. Second, under the existence of HSV antibodies, a recombinant HSV-1 vector might not be able to deliver transgenes into glioma cells. Herrlinger et al[25] reported that under preimmunization conditions, the HSV-1 vector was greatly, but not completely, reduced. Our newly developed HSV-1 helper/defective virus vector system should basically have high potential to strengthen replication-competent viral therapy strategy with HSV-1.

Replication-competent HSV-1 demonstrated cytotoxic effects and hTIMP-2-expressing defective particles showed the ability to inhibit the invasive activities of MMPs. Our results demonstrated that hTIMP-2 expressed by defective particles with a replication-competent helper virus had advantages of both cytotoxicity and invasion inhibition. The hTIMP-2-expressing replication-competent HSV-1 helper/defective system is expected to be clinically useful for the treatment of malignant brain tumors when generated with attenuated, multimutated HSV (e.g., HSV-G207), which replicates only in highly proliferating tumor cells *in vivo*.

ACKNOWLEDGMENTS

We are grateful to Dr. Motoharu Seiki (Department of Cancer Cell Research, Institute of Medical Science, University of Tokyo, Tokyo, Japan) for providing us with hTIMP-2 cDNA, Dr. Samuel D. Rabkin (Department of Neurosurgery, Georgetown University Medical Center, Washington, DC) for pSRa-ori4 amplicon plasmid, and Dr. John Subak-Sharpe (Institute of Virology, Glasgow, UK) for HSV-tsK. We also thank Dr. Robert L. Martuza (Department of Neurosurgery, Harvard Medical School and Massachusetts General Hospital, Boston, Mass) for scientific assistance and Kumiko Nakamura for secretarial assistance. This study was supported in part by a grant-in-aid for scientific research from the Ministry of Education, Science, Sports, and Culture of Japan, by grants from the Ministry of Health and Welfare of Japan, by a grant-in-aid from The Tokyo Biochemical Research Foundation, and by research grants for life sciences and medicine from The Keio University Medical Science Fund.

REFERENCES

1. Mineta T, Rabkin SD, Yazaki T, Hunter WD, Martuza RL. Attenuated multi-mutated herpes simplex virus-1 for the treatment of malignant gliomas. *Nat Med.* 1995;1:938–943.
2. Yazaki T, Manz HJ, Rabkin SD, Martuza RL. Treatment of human malignant meningiomas by G207, a replication-competent multimutated herpes simplex virus 1. *Cancer Res.* 1995;55:4752–4756.
3. Andersen J, Garber D, Meaney C, Breakefield X. Gene transfer into mammalian central nervous system using herpes simplex vectors: extended expression of bacterial *lacZ* in neurons using the neuron-specific enolase promoter. *Hum Gene Ther.* 1992;3:487–499.
4. Dobson A, Margolis TP, Sedarati F, Stevens J, Feldman LT. A latent, nonpathogenic HSV-1-derived vector stably expresses β-galactosidase in mouse neurons. *Neuron.* 1990; 5:353–360.
5. Fink D, Stenberg L, Weber P, Mata M, Gonis W, Glorioso J. In vivo expression of β-galactosidase in hippocampal neurons by HSV-1-mediated transfer. *Hum Gene Ther.* 1992;3:11–19.
6. Rutka JT, Matsuzawa K, Hubbard S, et al. Expression of TIMP-1, TIMP-2, 72-and 92-kDa type IV collagenase transcripts in human astrocytoma cell lines: correlation with astrocytoma cell invasiveness. *Int J Oncol.* 1995;6:877–884.
7. Abe T, Mori T, Kohno K, et al. Expression of 72-kDa type IV collagenase and invasion activity of human glioma cells. *Clin Exp Metastasis.* 1994;12:296–304.
8. Deryugina EI, Bourdon MA, Luo GX, Reisfeld RA, Strongin A. Matrix metalloproteinase-2 activation modulates glioma cell migration. *J Cell Sci.* 1997;110:2473–2482.
9. Nakano A, Tani E, Miyazaki K, Yamamoto Y, Furuyama J. Matrix metalloproteinases and tissue inhibitors of metalloproteinases in human gliomas. *J Neurosurg.* 1995;83: 298–307.
10. Nakagawa T, Kubota T, Kabuto M, Fujimoto N, Okada Y. Secretion of matrix metalloproteinase-2 (72-kDa gelatinase/type IV collagenase = gelatinase A) by malignant human glioma cell lines: implications for the growth and

cellular invasion of the extracellular matrix. *J Neurooncol.* 1996;28:13–24.
11. Sato H, Takino T, Okada Y, et al. A matrix metalloproteinase expressed in the surface of invasive tumour cells. *Nature.* 1994;37:61–65.
12. Rooprai HK, McCormick D. Proteases and their inhibitors in human brain tumours: a review. *Anticancer Res.* 1997; 17:4151–4162.
13. Zhang H, Kelly G, Zerillo C, Jaworski DM, Hockfield S. Expression of a cleaved brain-specific extracellular matrix protein mediates glioma cell invasion in vivo. *J Neurosci.* 1998;18:2370–2376.
14. Itoh Y, Ito A, Iwata K, Tanzawa K, Mori Y, Nagase H. Plasma membrane-bound tissue inhibitor of metalloproteinases (TIMP)-2 specifically inhibits matrix metalloproteinases 2 (gelatinase A) activated on the cell surface. *J Biol Chem.* 1998;38:24360–24367.
15. Lampert K, Machein U, Machein MG, Conca W, Peter HH, Volk B. Expression of matrix metalloproteinases and their tissue inhibitors in human brain tumors. *Am J Pathol.* 1998;153:429–437.
16. Nakagawa T, Kubota T, Kabuto M, Sato K, Kawano H, Hayakawa T, Okada Y. Production of matrix metalloproteinases and tissue inhibitor of metalloproteinases-1 by human brain tumors. *J Neurosurg.* 1994;81:69–77.
17. Kaplitt M, Peaus JG, Kleopoulos SP, Hanlon BA, Rabkin SD, Pfaff DW. Expression of a functional foreign gene in adult mammalian brain following in vivo transfer via a herpes simplex virus type 1-defective viral vector. *Mol Cell Neurosci.* 1991;2:320–330.
18. Rao JS, Steck PA, Mohanam S, Stetler-Stevenson WG, Liotta LA, Sawaya R. Elevated levels of M_r 92,000 type IV collagenases in human brain tumors. *Cancer Res.* 1993;53: 2208–2211.
19. Johnson P, Miyanohara A, Levine F, Cahill T, Friedman T. Cytotoxicity of replication-defective mutant of herpes simplex virus type 1. *J Virol.* 1992;66:2952–2965.
20. Marsden HS, Crombie IK, Subak-Sharpe JH. Control of protein synthesis in herpes virus-infected cells: analysis of the polypeptides induced by wild-type and sixteen temperature-sensitive mutants of HSV strain 17. *J Gen Virol.* 1976;31:347–372.
21. Davison MJ, Preston VG, McGeoch DJ. Determination of the sequence alternation in the DNA of the herpes simplex virus type 1 temperature-sensitive mutant tsK. *J Gen Virol.* 1984;65:859–863.
22. DeLuca N, McCarthy A, Schaffer P. Isolation and characterization of deletion mutants of herpes simplex virus type 1 in the gene encoding immediate-early regulatory protein ICP4. *J Virol.* 1985;56:558–570.
23. DeLuca N, Schaffer P. Activities of herpes simplex virus type 1 (HSV-1) ICP4 genes specifying nonsense peptides. *Nucleic Acids Res.* 1987;15:4491–4511.
24. Paterson T, Everett R. A prominent serine-rich region in Vmw175, the major transcriptional regulator protein of herpes simplex virus type 1, is not essential for virus growth in tissue culture. *J Gen Virol.* 1990;71:1775–1783.
25. Herrlinger U, Kramm CM, Aboody-Guterman KS, et al. Pre-existing herpes simplex virus 1 (HSV-1) immunity decreases, but does not abolish, gene transfer to experimental brain tumors by a HSV-1 vector. *Gene Ther.* 1998;5:809–819.

Exhibit 2

[CANCER RESEARCH 62, 7291–7297, December 15, 2002]

Inhibition of the Mammalian Target of Rapamycin Sensitizes U87 Xenografts to Fractionated Radiation Therapy[1]

Jeffrey S. Eshleman, Brett L. Carlson, Ann C. Mladek, Brian D. Kastner, Kathleen L. Shide, and Jann N. Sarkaria[2]

Department of Oncology, Mayo Clinic, Rochester, Minnesota 55905

ABSTRACT

The mammalian target of rapamycin (mTOR) modulates key signaling pathways that promote uncontrolled proliferation of glioblastoma multiforme (GBM). Because rapid tumor proliferation may contribute to the clinical radioresistance of GBM tumors, the combination of rapamycin, a selective mTOR inhibitor, and radiation was studied *in vitro* and *in vivo* in a GBM model. In monolayer cultures of U87 and SKMG-3 cells, rapamycin had no impact on radiation sensitivity. In contrast, rapamycin significantly enhanced the efficacy of fractionated radiation of established U87 xenografts in nude mice. Similar effects were seen in U87 spheroids treated with rapamycin and radiation, which suggests that the sensitizing effects of this drug are dependent on disruption of mTOR signaling pathways specifically within tumor cells. Inhibition of these signaling pathways can lead to inhibition of G_1-specific cyclin-dependent kinase activities, and this could contribute to the sensitizing effects of rapamycin. Consistent with this idea, roscovitine, a specific cyclin-dependent kinase inhibitor, also enhanced the efficacy of fractionated radiation in U87 spheroids. These data demonstrate that inhibition of tumor proliferation does not diminish the efficacy of fractionated radiation and suggest that disruption of key signal transduction pathways may significantly enhance the effectiveness of radiation therapy in malignant gliomas.

INTRODUCTION

GBM[3] is the most common primary central nervous system tumor in adults and is uniformly fatal despite aggressive therapy. Intensive research over the past three decades has focused on combining different cytotoxic chemotherapies with radiation in an effort to improve survival. Unfortunately, these approaches have had no impact on treatment outcome, and the standard of care continues to be surgical resection followed by external beam radiation therapy. GBMs are clinically radioresistant, and the majority of tumors recur within or at the margin of the radiation field. Biological factors in GBM that may contribute to this clinical radioresistance include intrinsic cellular radioresistance, rapid proliferative rate, invasiveness, and tumor hypoxia (1–6). With an increasing understanding of the cellular and molecular mechanisms governing these processes, combining radiation therapy with novel therapeutic agents specifically targeting one or more of these factors holds promise for improving the outcome of therapy in this difficult disease.

The mTOR is a key signaling molecule in GBM that drives uncontrolled tumor proliferation. mTOR is a serine-threonine kinase that functions downstream from Akt in a phosphatidylinositol 3′-kinase/Akt/mTOR signaling pathway. This pathway is commonly activated in GBM through constitutive activation of upstream receptor tyrosine kinases, such as epidermal growth factor receptor, and/or loss of PTEN tumor suppressor function (7–11). In response to mitogenic stimuli, mTOR regulates the phosphorylation of p70 S6 kinase and eIF4E-binding protein 1, which promotes translation of select mRNA transcripts (reviewed in Ref. 12). Selective inhibition of mTOR by the macrolide antibiotic rapamycin blocks phosphorylation of these two regulatory proteins and leads to cell cycle arrest through up-regulation of $p27^{kip1}$, a CDK inhibitor, and down-regulation of cyclin D1 (13–15). Rapamycin inhibits mTOR signaling at low nanomolar concentrations only when it is bound in a complex with the endogenous FK506-binding protein FKBP-12. The interaction of the FKBP12-rapamycin complex with mTOR is highly specific, and therefore cellular and biochemical effects of rapamycin are generally believed to result exclusively from inhibition of mTOR signaling (16, 17).

Rapamycin is well tolerated in patients and is a Food and Drug Administration-approved immunosuppressant for the prevention of solid organ transplant rejection (18). Screening by the National Cancer Institute revealed that rapamycin potently inhibited cell proliferation in a number of tumor types including prostate, breast, and glioblastoma cell lines. Rapamycin also inhibited tumor growth in animals, and these observations prompted the development of two rapamycin analogues, CCI-779 and RAD001, which currently are being evaluated in early clinical trials as anticancer agents. Anecdotal experience with CCI-779 in these trials suggests promising activity in several tumor types including malignant gliomas.

Proliferation of tumor cells during a 6- or 7-week course of radiation therapy can repopulate a tumor and decrease the efficacy of radiation treatment (19, 20). This suggests that pharmacological inhibition of tumor repopulation with a cytostatic agent might enhance the overall efficacy of fractionated radiation (21). However, growth-arrested cells held in confluence can be more radioresistant than actively cycling cells (22), which suggests that cytostatic agents might actually increase the radiation resistance of tumors. To test these potentially conflicting hypotheses, the effects of rapamycin on radiation response were evaluated both *in vitro* and *in vivo*. In monolayer culture, rapamycin inhibited proliferation of U87 and SKMG-3 malignant glioma cell lines without any significant change in radioresistance. In contrast, rapamycin treatment significantly enhanced the efficacy of fractionated radiation in U87 flank xenografts. Consistent with inhibition of repopulation, rapamycin treatment decreased tumor proliferation in these xenografts. Moreover, similar "sensitization" was observed in U87 spheroids treated *in vitro* with fractionated radiation in the presence of either rapamycin or the selective cell cycle inhibitor roscovitine. These studies suggest that novel cell cycle inhibitors might be used in combination with fractionated radiation therapy to inhibit tumor repopulation and improve local tumor control.

MATERIALS AND METHODS

Cell Culture and Antibodies. A172, U87, and U118 malignant glioma cell lines were maintained in DMEM (Life Technologies, Inc.), and SKMG-3 cells were maintained in α-MEM (BioWhitaker), respectively. Both media were supplemented with 10% fetal bovine serum and 10 mM HEPES. Cell lines were obtained from Dr. C. David James. Rapamycin (NSC 226080) was obtained

Received 6/10/02; accepted 10/10/02.

The costs of publication of this article were defrayed in part by the payment of page charges. This article must therefore be hereby marked *advertisement* in accordance with 18 U.S.C. Section 1734 solely to indicate this fact.

[1] Supported by the Mayo Foundation, Mayo Cancer Center, and NIH Grant CA80829 (to J. N. S.).

[2] To whom requests for reprints should be addressed, at Department of Oncology, Mayo Clinic, Rochester, MN 55905.

[3] The abbreviations used are: GBM, glioblastoma multiforme; mTOR, mammalian target of rapamycin; MTS, (3-(4,5-dimethylthiazol-2-yl)-5-(3-carboxymethoxyphenyl)-2-(4-sulfophenyl)-2H-tetrazolium salt; BrdUrd, bromodeoxyuridine; CI, confidence interval; CDK, cyclin-dependent kinase; VEGF, vascular endothelial growth factor.

from the National Cancer Institute Developmental Therapeutics Program[4] and dissolved in ethanol to yield a 5 mg/ml stock solution, which was stored at −20°C. The drug was diluted in media immediately before treatment of cells. Antibodies specific for p70 S6 kinase were obtained from Santa Cruz Biotechnology (sc-230) and Cell Signaling (catalogue number 9202). An antibody that specifically recognized phosphorylation of p70 S6 kinase on Thr-389 was obtained from Cell Signaling (catalogue number 9205).

Immunoprecipitation and Western Blotting. Cells cultured in 100-mm tissue culture dishes were harvested for assays during exponential growth. The cells were washed twice with PBS and then scraped on ice in 1 ml of lysis buffer [25 mM Tris, 50 mM NaCl, 10% glycerol, and 1% Triton X-100 (pH 7.4) containing 50 mM β-glycerol phosphate, 10 μg/ml aprotinin, 5 μg/ml pepstatin, 10 μg/ml leupeptin, and 20 nM microcystin].

Lysates were cleared of insoluble material by centrifugation, and equivalent amounts of protein (1 mg) were incubated on ice for 30 min with p70 S6 kinase-specific antibodies (Santa Cruz Biotechnology). The immune complexes were precipitated with protein A-Sepharose beads, and the resulting immunoprecipitates were washed twice in lysis buffer. Samples were boiled in 1× SDS sample buffer, resolved by SDS-PAGE, and transferred to Immobilon-P membranes (Millipore). Membranes were probed with 1 μg/ml phospho-specific Thr-389 antibody diluted in Tris-buffered saline containing 0.02% Tween 20 and 5% nonfat dried milk. After washing in Tris-buffered saline containing 0.02% Tween 20, membranes were incubated with a secondary polyclonal rabbit antimouse IgG antibody conjugated to horseradish peroxidase (Cell Signaling). Membranes were developed with Super Signal Chemiluminescence reagent (Pierce). Finally, the blots were stripped and reprobed with non-phospho-specific p70 S6 kinase antibodies (Cell Signaling).

Clonogenic Assay. The effect of rapamycin on the radiosensitivity of U87 and SKMG-3 cells was assessed in a clonogenic assay. Cells were treated with 0 or 100 nM rapamycin diluted in media for 24 h before trypsinization and resuspension in fresh growth medium. Portions of the cells were processed for cell cycle analysis, whereas the remaining cells were treated in a clonogenic assay. Cells were irradiated with a ^{137}Cs source at a dose rate of 6.4 Gy/min in suspension culture and immediately plated in triplicate 60-mm dishes at cell concentrations estimated to yield 20–100 colonies/dish. To maximize plating efficiency, up to 50,000 lethally irradiated U87 feeder cells were added to the U87 plates (plating efficiency, 9%). No feeder cells were required for the SKMG-3 cells (plating efficiency, 34%). The final concentration of ethanol, used as the drug solvent, did not exceed 0.1% (v/v), and this solvent concentration had no effect on either the clonogenicity or radiosensitivity of either cell line (data not shown). Cells were cultured for 2 weeks before fixation and staining with Coomassie Blue. Colonies with >50 cells were scored.

MTS Assay. Cells in exponential growth were harvested and plated in 96-well plates (1500 cells/well in 80 μl of standard growth medium). Each treatment condition was tested in six replicate wells. Cells were incubated overnight, and then graded concentrations of rapamycin were added to the wells in 20 μl of media. Cells were incubated at 37°C for 72 h and then processed for the MTS assay (Promega) according to the manufacturer's instructions. After incubation of cells with the MTS reagent for 2 h, absorbance at 490 nm was measured in a spectrophotometer.

Cell Cycle Analysis. Cells were fixed in 70% ethanol diluted in PBS, and the samples were stored at −20°C. The fixed cells were resuspended in PBS containing 20 μg/ml propidium iodide and 100 μg/ml boiled RNase A and incubated for 30 min at 37°C before flow cytometric analysis on a Becton Dickinson FACScan. Twenty-thousand ungated events were collected. Cell cycle distribution was determined using the ModFit software package (Verity) after excluding doublets and clumps by gating on the DNA pulse-width *versus* pulse-area displays. To measure BrdUrd incorporation, animals received an i.p. injection of 1 mg of BrdUrd 30 min before euthanasia. Tumors were removed from the animals, diced into small pieces, and fixed in 70% ethanol diluted in PBS. Samples were processed for flow cytometry as described previously and analyzed on a Becton Dickinson FACScan (23). After excluding clumps and doublets, a bivariate distribution of green height (BrdUrd-FITC) and red area (cell cycle/propidium iodide) was analyzed to quantitate the fraction of BrdUrd-positive nuclei.

[4] http://dtp.nci.nih.gov/docs/misc/available_samples/dtp_indsamples.html.

Regrowth Delay Assay. Flank xenografts were established in 8–10-week-old female athymic nude mice by s.c. injection of 2–5 million U87 cells resuspended in 50 μl of media. Approximately 4 weeks after injection, animals with established xenografts were stratified by size and randomized into four treatment groups: (*a*) control; (*b*) radiation only; (*c*) rapamycin only; and (*d*) rapamycin + radiation. For irradiation, unanesthetized animals were immobilized in a lead jig that shielded the head, thorax, and upper abdomen. Radiation was delivered at a dose rate of 4 Gy/min through a single posterior to anterior 300 kVp unfiltered photon beam (half-value layer, 2.73 mm Al). For rapamycin injections, stock rapamycin was diluted first in sterile 10% PEG400/8% ethanol and then in an equal volume of sterile 10% Tween 80 for a final concentration of 20 μg rapamycin/100 μl. Rapamycin was delivered by i.p. injection, and the doses of rapamycin were calculated assuming that all mice weighed 20 g. Tumors were measured with calipers in three dimensions, 3–5 times/week. Tumor volume was calculated using the formula for volume of an ellipsoid: $4/3\pi \times L/2 \times W/2 \times H/2$, where L = length, W = width, and H = height. Time for tumor regrowth to three times the initial volume was calculated for each animal. Regrowth delay was calculated as the difference in the mean regrowth times for any pair of treatments.

Spheroid Culture. U87 cells were initially plated on Petri dishes to induce spheroid formation and subsequently transferred to spinner flasks. Cultures were stirred continuously for 4–7 days. For the regrowth delay experiments, single spheroids were transferred to individual wells of a multiwell plate that had been previously coated with 1% agarose dissolved in DMEM. The indicated drug concentrations were added 1 h before irradiation. Spheroids were irradiated in air at room temperature as described above for the radiation clonogenic assays. Spheroids were measured in two dimensions 3×/week using an optical micrometer in an inverted light microscope. The volume of a spheroid was estimated using the formula $4/3\pi \times L/2 \times W/2 \times W/2$, where the width, W, is the shorter of the two dimensions. The time for spheroid regrowth to 10 times initial volume was calculated for each spheroid. Regrowth delay is calculated as the difference in the mean regrowth times for any pair of treatments.

Statistics. A two-tailed Student's t test was used to establish statistical significance between control and rapamycin treatment for the MTS and flow cytometry data. Results from two independent animal regrowth delay experiments were pooled for statistical analysis. CIs for the regrowth delay were calculated based on a pooled estimator of variance (s_p^2) using the following formula: $CI = t \times s_p \times (1/n_1 + 1/n_2)^{-2}$, where t is obtained from a t-distribution with $(n_1 + n_2 - 2)$ degrees of freedom. Data from the spheroid regrowth delay assays were handled in a similar manner. Data from two independent determinations of BrdUrd labeling index were pooled, and Wilcoxon's rank-sum test was used to test the difference between rapamycin and control treatment.

RESULTS

Rapamycin Inhibits Cell Proliferation *in Vitro*. The effects of rapamycin on proliferation were examined in four glioma cell lines using a MTS assay. This assay relies on the bioreduction of a tetrazolium compound by metabolically active cells into a soluble formazan salt, which then can be quantitated using a spectrophotometer. As seen in Fig. 1*A*, incubation with 100 nM rapamycin for 72 h significantly inhibited the proliferation of A172, SKMG-3, U87, and U118 cells. Based on these data, we elected to study the effects of rapamycin on SKMG-3 and U87 cells in more detail. The observed decrease in proliferation after treatment with 100 nM rapamycin corresponded with a significant accumulation of cells in the G_0-G_1 compartment ($P < 0.001$), as early as 24 h after drug addition, and a corresponding decrease in the fraction of cells traversing S phase ($P < 0.001$; Fig. 1*B*). Consistent with a noncytotoxic mechanism of action, rapamycin did not induce apoptosis or diminish clonogenic cell survival (data not shown).

Rapamycin Does Not Affect Radiation Sensitivity *in Vitro*. Classic radiobiological studies have demonstrated that noncycling cells can be relatively radioresistant (22, 24). This suggests that combining a cytostatic agent with radiation might actually increase the radiation resistance of tumor cells. To address this concern di-

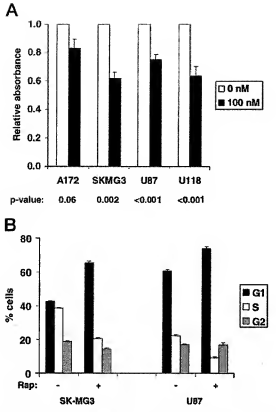

Fig. 1. Rapamycin inhibits proliferation. *A*, A172, SKMG-3, U87, and U118 cells were incubated with 0 or 100 nM rapamycin for 72 h and then processed in a MTS assay. In this assay, absorbance at a wavelength of 490 nm is proportional to cell number. The absorbance for drug-treated cells was normalized to that of control-treated cells, and the results shown represent the mean ± SE from four independent experiments. *B*, cells were incubated with 0 or 100 nM rapamycin for 24 h, and the cell cycle distribution was determined by flow cytometric analysis. Results shown represent the mean ± SE of triplicate samples from a single experiment. Identical results were obtained in three independent experiments. The effects of rapamycin on the distribution of cells in G_0-G_1 and S phase were statistically significantly for both cell lines ($P < 0.001$).

rectly, U87 and SKMG-3 cells were incubated with 100 nM rapamycin for 24 h and then simultaneously processed for flow cytometric analysis and radiation clonogenic survival assays. As shown in Figs. 2, *A* and *B*, preincubation with rapamycin had no effect on radiation survival of U87 and SKMG-3 cells, despite accumulation of cells in G_0-G_1 and a corresponding decrease in the S-phase fraction. The results in SKMG-3 cells are especially noteworthy in that rapamycin treatment caused a marked G_0-G_1 arrest and yet had absolutely no effect on radiation sensitivity compared with control-treated cells. Similar results were obtained with U251, A172, and U118 malignant glioma cell lines, and incubation of cells with rapamycin after irradiation also had no effect on radiosensitivity (data not shown). Taken together, these data indicate that rapamycin-induced cell cycle arrest does not increase the radioresistance of glioma cell lines growing in monolayer culture.

Rapamycin-mediated Inhibition of mTOR Signaling. The planned combination studies with rapamycin and radiation required identification of a rapamycin dosing regimen that inhibits mTOR signaling in xenografts. Because SKMG-3 cells are not tumorigenic in nude mice, these experiments were performed in U87 cells. Previous studies suggest that the rapamycin-FKBP12-mTOR complex is extremely stable and that rapamycin is essentially an irreversible inhibitor of mTOR (25). Consistent with these results, incubation of U87 cells with 10 nM rapamycin for 1 h completely inhibited mTOR-dependent phosphorylation of p70 S6 kinase (Fig. 3*A*), and mTOR signaling remained completely inhibited for at least 72 h after replacement of the drug-containing media with fresh media. Using a similar approach, the dose of rapamycin required to inhibit mTOR signaling in established U87 xenografts was identified. The i.p. injection of either 0.1 or 1 mg/kg rapamycin resulted in complete inhibition of p70 S6 kinase phosphorylation 24 h after drug treatment (Fig. 3*B*). These data suggest that adequate inhibition of mTOR signaling would be achieved by intermittent dosing with 1 mg/kg rapamycin delivered by i.p. injection once every 3 days.

Rapamycin Enhances the Efficacy of Radiation in U87 Xenografts. Proliferation of tumor cell clonogens between radiation doses can significantly affect the overall efficacy of therapy (19, 20). Rapamycin inhibits proliferation of U87 cells, and the rapamycin-induced cell cycle arrest does not increase the radioresistance of these cells. Therefore, we hypothesized that the combination of rapamycin with fractionated radiation therapy should improve the efficacy of treatment of U87 tumors. This hypothesis was tested in a tumor regrowth delay assay using U87 flank xenografts grown in nude mice. Because tumor proliferation between radiation fractions was of specific interest, radiation was given in a protracted schedule of four fractions delivered in a total of 18 days (Fig. 4*A*). Based on our mTOR inhibition studies, rapamycin (1 mg/kg) was delivered once every 3 days by i.p. injection throughout the course of radiation. To ensure that mTOR would be fully inhibited at the

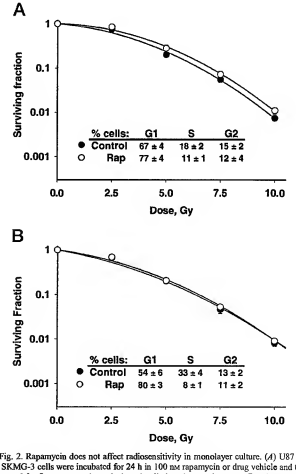

Fig. 2. Rapamycin does not affect radiosensitivity in monolayer culture. (*A*) U87 and (*B*) SKMG-3 cells were incubated for 24 h in 100 nM rapamycin or drug vehicle and then processed for flow cytometric analysis and radiation clonogenic assays. Results represent the combined data from three independent experiments, with individual data points representing the mean ± SE survival (error bars are obscured by symbols for most points). The cell cycle distribution of control and rapamycin-treated cells from these same experiments is shown (mean ± SE).

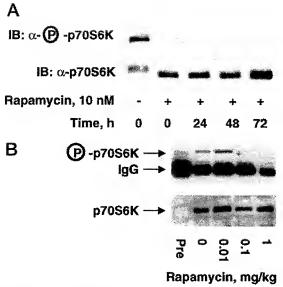

Fig. 3. Dosing schedule determination for rapamycin. *A*, U87 cells were incubated with 0 or 10 nM rapamycin for 1 h, and then the drug-containing media were washed off and replaced with fresh media. At the indicated time points after removal of the rapamycin, cells were snap-frozen and stored at −80°C. Frozen cell pellets were lysed, and p70 S6 kinase was immunoprecipitated. After SDS-PAGE and electrotransfer, nylon membranes were probed with phospho-Thr-389-specific p70 S6 kinase antisera. The membrane was stripped and reprobed with p70 S6 kinase antisera. Identical results were obtained in two independent experiments. *B*, the indicated doses of rapamycin were injected i.p. into nude mice with established U87 flank xenografts. Animals were euthanized 24 h later, and the tumors were processed as described above for determination of p70 S6 kinase phosphorylation status.

time of irradiation, rapamycin was administered 1 day before radiation. Animals with established U87 s.c. flank xenografts were randomized into four treatment groups: (*a*) control; (*b*) radiation only; (*c*) rapamycin only; and (*d*) rapamycin plus radiation. During and after treatment, tumors were measured in three dimensions, and the relative tumor volume was tracked for each animal.

The results from a representative xenograft experiment are presented in Fig. 4*B*. Identical results were obtained in a second experiment, and the data from the two experiments were pooled for an analysis of tumor regrowth delay after radiation. Control-treated tumors grew rapidly, with a volume doubling time of approximately 5 days. Compared with control, radiation therapy alone (16 Gy over 18 days) was ineffective and had no effect on tumor growth (regrowth delay of −0.2 ± 4.6 days; mean ± 95% CI). This result is consistent with reports that U87 flank xenografts are highly radioresistant; a single dose of 51.9 Gy is required to cure 50% of established flank U87 xenografts (1). The relatively low-intensity rapamycin dosing schedule also did not have significant effects on overall tumor growth rates. However, rapamycin significantly enhanced the efficacy of radiation; the combination of rapamycin with radiation resulted in a regrowth delay of 19.1 ± 6.3 days compared with treatment with rapamycin alone. Thus, combination therapy with rapamycin and radiation was significantly more effective than either radiation alone or rapamycin alone.

Rapamycin Reduces Tumor Cell Proliferation *in Vivo*. Tumor repopulation between radiation fractions also can lead to significant loss in treatment efficacy. To assess whether the dosing schedule of rapamycin used in the regrowth experiments was sufficient to inhibit tumor proliferation, the fraction of cells in S phase was determined in tumor-bearing animals treated with or without three doses of rapamycin delivered once every 3 days. Twenty-four h after the last drug dose, animals were injected with 1 mg of BrdUrd 30 min before euthanasia. BrdUrd is a thymidine analogue that is incorporated into DNA during S phase, and cells containing BrdUrd-labeled DNA were quantitated using a flow cytometric technique. Two independent experiments were performed, and the results are shown in Fig. 5. In both experiments, rapamycin treatment decreased BrdUrd labeling. Pooling the data from the two experiments for analysis, the median labeling index decreased by nearly 50% (P = 0.02, Wilcoxon's rank-sum test). Overall, the labeling indices were higher for both

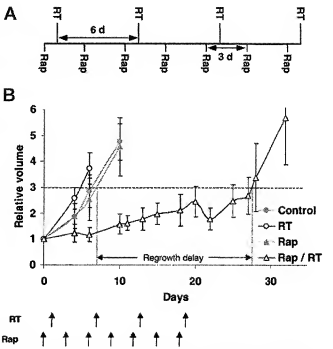

Fig. 4. Rapamycin sensitizes U87 xenografts *in vivo*. Nude mice with established U87 flank xenografts were randomized into four treatment groups: (*a*) placebo; (*b*) radiation only (4 Gy × 4); (*c*) rapamycin only (1 mg/kg); or (*d*) radiation and rapamycin. *A*, the schedule for rapamycin (*Rap*) and radiation treatment (*RT*) is depicted. *B*, the tumor regrowth for each treatment group is shown. Data points represent the mean relative tumor volume ± SE. Treatment was initiated on day 0 with the first injection of rapamycin (*Rap*). The schedule for rapamycin and radiation (*RT*) treatments is depicted below the *X* axis. Identical results were obtained in two independent experiments.

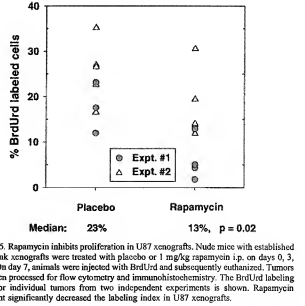

Fig. 5. Rapamycin inhibits proliferation in U87 xenografts. Nude mice with established U87 flank xenografts were treated with placebo or 1 mg/kg rapamycin i.p. on days 0, 3, and 6. On day 7, animals were injected with BrdUrd and subsequently euthanized. Tumors were then processed for flow cytometry and immunohistochemistry. The BrdUrd labeling index for individual tumors from two independent experiments is shown. Rapamycin treatment significantly decreased the labeling index in U87 xenografts.

control- and drug-treated groups in the second experiment, and this appeared to be related to tumor size. After accounting for tumor size in a multivariate statistical analysis, rapamycin treatment remained the most significant factor influencing labeling index ($P = 0.003$). Interestingly, this rapamycin-mediated cell cycle arrest in the xenografts translated into only a slightly longer tumor regrowth time for the rapamycin-treated animals (9.7 ± 2.3 days) compared with control-treated animals (8.6 ± 1.5 days). Nonetheless, these *in vivo* cell cycle arrest data are consistent with biochemical inhibition of mTOR activity by rapamycin demonstrated in Fig. 3*B* and are similar in magnitude to that seen in U87 cells after *in vitro* rapamycin treatment (Fig. 1*B*).

Rapamycin Sensitizes U87 Spheroids to Radiation. In addition to effects on tumor cell death or proliferation, rapamycin could affect host-tumor interactions, such as angiogenesis, cytokine production, or immune responses, that could influence the response to fractionated radiation. To distinguish between tumor-specific and host-specific effects of rapamycin, the response of U87 spheroids to fractionated radiation therapy was assessed in the presence and absence of rapamycin. U87 cells grown on untreated Petri dishes spontaneously form spheroids, and the response of spheroids to therapy can be tracked over time using a regrowth delay assay (26, 27). Diffusion gradients of oxygen and nutrients occur within multicellular spheroids, with low-oxygen, poor-nutrient conditions existing toward the center (28). As in solid tumors, these nutrient and oxygen gradients result in subpopulations of proliferating, quiescent, hypoxic, and anoxic tumor cells that each respond differently to radiation. Distinct from solid tumors grown in nude mice, multicellular spheroids lack key tumor components derived from host tissues that can affect treatment efficacy, such as supporting stromal cells, a vascular supply, and humoral antitumor immunity. Therefore, any effect of rapamycin on radiation response in a spheroid system must be due to the effects of rapamycin on tumor cells and would suggest that at least part of the radiosensitizing effects of rapamycin in animals are host independent.

The effects of rapamycin and radiation on spheroid growth were evaluated in regrowth delay assays that were similar to those used in the earlier animal studies. As in the xenograft studies, groups of randomly selected spheroids were treated with (*a*) vehicle control, (*b*) fractionated radiation (2 Gy × 4), (*c*) 10 nM rapamycin, or (*d*) rapamycin plus radiation. Because the volume doubling time for untreated spheroids was half that of the U87 flank xenografts, the overall length of the radiation fractionation schema was reduced to 9 days. Representative results from a single experiment are shown in Fig. 6*A*, and data from three independent experiments were pooled for statistical analysis of the regrowth delay. Similar to the animal studies, radiation alone had minimal effect on spheroid growth compared with control treatment (regrowth delay of 4.2 ± 2.6 days, mean ± 95% CI), whereas rapamycin alone had a more dramatic effect compared with control (regrowth delay = 13.5 ± 1.7 days). Presumably, the more profound growth-inhibitory effects of rapamycin in the spheroids compared with the animal studies reflect higher intratumoral drug concentrations in the spheroids *versus* the xenografts. As in the animal studies, the combination of rapamycin with radiation was significantly more effective than treatment with rapamycin alone (growth delay = 11.9 ± 3.6 days). These results are qualitatively similar to those seen in the U87 xenograft combination studies and suggest that the mechanism of rapamycin-mediated radiation "sensitization" is dependent, in part, on inhibition of mTOR signaling within tumor cells.

The animal and spheroid data are both consistent with the hypothesis that inhibition of tumor repopulation may contribute to the sensitizing effects of this drug in combination with radiation. If this is true, then another cytostatic agent with a completely distinct mechanism of action should have similar effects when combined with radiation. Therefore, we evaluated the combination of radiation with roscovitine in U87 spheroids. Roscovitine is a purine analogue that selectively inhibits CDKs 1, 2, and 5 and currently is in early clinical trials as an antitumor agent (29). In a regrowth delay assay similar to those performed previously, the effects of radiation alone on spheroid regrowth were more variable compared to control treatment with a growth delay of 15.7 ± 11.8 days (Fig. 6*B*). However, the combination of roscovitine with radiation was significantly more effective than roscovitine alone with an associated regrowth delay of 23.8 ± 7.0 days. These results are similar to those seen with the combination of rapamycin and radiation and suggest that both drugs have at least additive effects when combined with radiation in a spheroid model. Thus, inhibition of tumor proliferation during fractionated radiation therapy may enhance the efficacy of treatment, and the radiosensitizing effects of rapamycin in xenograft and spheroid models may be due partially to inhibition of tumor repopulation.

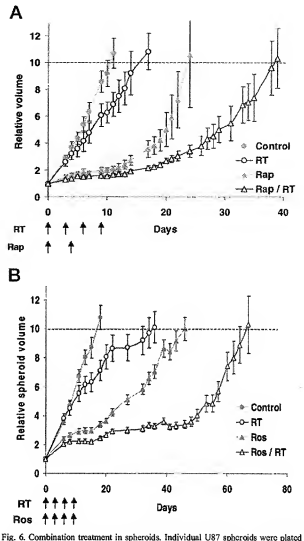

Fig. 6. Combination treatment in spheroids. Individual U87 spheroids were plated in multiwell plates and divided into four treatment groups as described in the Fig. 5 legend. In the indicated treatment groups, four fractions of 2 Gy radiation (*RT*) were delivered over a 9-day period (day 0, 3, 6, and 9). In *A*, 10 nM rapamycin was added to the culture media 30 min before radiation on day 0, and rapamycin-containing media were replenished on day 4. For roscovitine treatment (*B*), media containing 30 μM roscovitine were added 30 min before each radiation treatment (days 0, 3, 6, and 9). The regrowth for each treatment group is shown with data points representing the mean relative spheroid volume ± SE. Similar results were obtained in at least two independent experiments for each treatment condition.

DISCUSSION

Tumor proliferation during fractionated radiation is a major detrimental factor influencing local tumor control. After a dose of radiation, surviving tumor clonogens continue to proliferate and repopulate the tumor. During the latter half of a 6- or 7-week clinical course of therapy, the proliferation rate increases so that one-third to one-fourth of a typical 2-Gy radiation dose is required each day just to sterilize newly formed tumor cells (19). Moreover, tumor proliferation during extended treatment breaks is associated with a 10–15% loss in local control for each week of treatment prolongation (30). These observations suggest that pharmacological inhibition of tumor repopulation could have profound clinical impact on local tumor control. In the present study, the novel therapeutic agent rapamycin, a selective inhibitor of mTOR, was evaluated in combination with radiation both *in vitro* and *in vivo*. Rapamycin had no effect on the intrinsic radiation sensitivity of cells grown in monolayer culture, whereas rapamycin profoundly enhanced the efficacy of fractionated radiotherapy in xenografts. Although multiple mechanisms may contribute to rapamycin-mediated sensitization, the recapitulation of this phenomenon in tumor spheroids treated with either rapamycin or a selective CDK inhibitor suggests that inhibition of proliferation may contribute to this effect.

Pharmacological manipulation of tumor repopulation has been effectively combined with radiation in several model systems. We initially demonstrated the proof of principle for this concept in an estrogen-dependent MCF-7 xenograft model where tumor proliferation rates could be hormonally manipulated. In this system, removing an exogenous estrogen source during treatment slowed tumor proliferation and ameliorated the adverse effects of treatment prolongation (23, 31). The current study extends this idea by demonstrating that selective disruption of key signaling pathways important for cell growth and proliferation in U87 xenografts significantly enhances the efficacy of fractionated radiation. Similar to these results, selective inhibition of epidermal growth factor receptor signaling sensitizes squamous cell carcinoma xenografts to fractionated radiation (reviewed in Ref. 32). The observation that either rapamycin or roscovitine, a selective CDK inhibitor, enhances the efficacy of fractionated radiation therapy in an *in vitro* spheroid model bolsters the idea that inhibition of tumor proliferation can improve the efficacy of fractionated radiotherapy. Whether this effect results specifically from inhibition of tumor repopulation (tumor clonogen proliferation between radiation fractions) or from a decreased ability of tumor cells to proliferate after the completion of radiation treatment is an unresolved issue. Future experiments are planned to explore this issue by comparing the sensitizing effects of rapamycin in animals treated with radiation in a short (3-day) *versus* long (18-day) fractionation schedule.

The sensitizing effects of rapamycin in the U87 xenograft and spheroid models are quite striking in comparison with the complete lack of effect of rapamycin in the radiation clonogenic survival assays. In combination with previously published reports, these data demonstrate that rapamycin does not affect the intrinsic radiosensitivity of cells and does not act as a "classic" radiosensitizing agent (33). As discussed above, the effects of rapamycin on tumor repopulation may contribute to these disparate results. However, the *in vivo* effects of rapamycin on tumor proliferation are relatively modest (Fig. 5) compared with the profound sensitizing effects of the drug in the xenograft regrowth delay assay (Fig. 4*B*). This suggests that other factors also may be important for the sensitizing effects of rapamycin. For example, rapamycin induces significant changes in glucose and nitrogen metabolism, and the starvation-like metabolic state induced by rapamycin potentially could decrease oxygen consumption in solid tumors and improve overall tumor oxygenation (34). Any decrease in the proportion of radioresistant hypoxic cells should significantly increase the efficacy of radiation. Studies currently are under way to evaluate the effects of rapamycin on hypoxia in U87 xenografts, and the potential importance of drug-induced changes in tumor oxygenation could be evaluated by comparing the sensitizing effects of rapamycin in tumors irradiated under clamped hypoxic conditions *versus* unclamped normoxic conditions.

The present results do not exclude the possibility that rapamycin also might inhibit host-dependent processes that contribute to the profound sensitizing effects of rapamycin in the xenograft model. Rapamycin is a potent inhibitor of endothelial cell proliferation *in vitro,* and systemic administration of rapamycin can inhibit angiogenesis (35). These effects are mediated primarily through modulation of VEGF-dependent signaling, with rapamycin inhibiting both hypoxia-inducible VEGF expression and downstream signaling from the VEGF receptor (36–38). Several studies have demonstrated that angiogenesis inhibitors targeting VEGF signaling pathways sensitize tumors to radiation in xenograft systems (39–42). Taken together, these observations suggest that an antiangiogenic effect of rapamycin might enhance the efficacy of radiation. However, in the current study, rapamycin did not have a significant effect on the density of CD31-positive microvessels in established U87 xenografts (data not shown), but additional studies will be required to determine whether the rapamycin dosing schedule used was adequate to suppress VEGF expression or VEGF receptor signaling.

Molecularly targeted therapeutics are being developed against numerous cell cycle-regulatory pathways and potentially could be combined with radiation to inhibit tumor repopulation in various tumor types. To maximize radiosensitization, the selection of a therapeutic agent should be based on the identification of the operant signaling pathways driving proliferation in a specific tumor. However, cell cycle-regulatory pathways also drive stem cell repopulation in many epithelial normal tissues in response to radiation injury. Therefore, selective inhibition of repopulation should target pathways that are selectively deregulated in tumor tissues compared with normal tissues. Little is known about the molecular and cellular mechanisms responsible for radiation-induced damage in normal brain, but the paucity of rapidly proliferating tissues suggests that cell cycle-directed therapeutics may not significantly increase radiation-induced central nervous system toxicities. Selective inhibition of mTOR by the novel therapeutic rapamycin profoundly sensitizes U87 xenografts to radiation, and this demonstration provides a strong rationale for the clinical evaluation of the combination of rapamycin and radiation in patients with GBM.

ACKNOWLEDGMENTS

We thank Drs. Robert Abraham, Larry Karnitz, and Junjie Chen for invaluable discussions and critical review of the manuscript. Dr. Patrick Roche, Dr. Marie-Christine Aubry, James Tarara, and members of the Mayo Cancer Center Flow Cytometry Laboratory and Immunohistochemistry Laboratory provided expert technical assistance.

REFERENCES

1. Suit, H. D., Zietman, A., Tomkinson, K., Ramsay, J., Gerweck, L., and Sedlacek, R. Radiation response of xenografts of a human squamous cell carcinoma and a glioblastoma multiforme: a progress report. Int. J. Radiat. Oncol. Biol. Phys., *18:* 365–373, 1990.
2. Taghian, A., DuBois, W., Budach, W., Baumann, M., Freeman, J., and Suit, H. *In vivo* radiation sensitivity of glioblastoma multiforme. Int. J. Radiat. Oncol. Biol. Phys., *32:* 99–104, 1995.
3. Labrousse, F., Daumas-Duport, C., Batorski, L., and Hoshino, T. Histological grading and bromodeoxyuridine labeling index of astrocytomas. Comparative study in a series of 60 cases. J. Neurosurg., *75:* 202–205, 1991.

4. Onda, K., Davis, R. L., Shibuya, M., Wilson, C. B., and Hoshino, T. Correlation between the bromodeoxyuridine labeling index and the MIB-1 and Ki-67 proliferating cell indices in cerebral gliomas. Cancer (Phila.), *74:* 1921–1926, 1994.
5. Rampling, R., Cruickshank, G., Lewis, A. D., Fitzsimmons, S. A., and Workman, P. Direct measurement of pO$_2$ distribution and bioreductive enzymes in human malignant brain tumors. Int. J. Radiat. Oncol. Biol. Phys., *29:* 427–431, 1994.
6. Maher, E. A., Furnari, F. B., Bachoo, R. M., Rowitch, D. H., Louis, D. N., Cavenee, W. K., and DePinho, R. A. Malignant glioma: genetics and biology of a grave matter. Genes Dev., *15:* 1311–1333, 2001.
7. Sekulic, A., Hudson, C. C., Homme, J. L., Yin, P., Otterness, D. M., Karnitz, L. M., and Abraham, R. T. A direct linkage between the phosphoinositide 3-kinase-AKT signaling pathway and the mammalian target of rapamycin in mitogen-stimulated and transformed cells. Cancer Res., *60:* 3504–3513, 2000.
8. Holland, E. C., Celestino, J., Dai, C., Schaefer, L., Sawaya, R. E., and Fuller, G. N. Combined activation of Ras and Akt in neural progenitors induces glioblastoma formation in mice. Nat. Genet., *25:* 55–57, 2000.
9. Frederick, L., Wang, X. Y., Eley, G., and James, C. D. Diversity and frequency of epidermal growth factor receptor mutations in human glioblastomas. Cancer Res., *60:* 1383–1387, 2000.
10. Ishii, N., Maier, D., Merlo, A., Tada, M., Sawamura, Y., Diserens, A. C., and Van Meir, E. G. Frequent co-alterations of TP53, p16/CDKN2A, p14ARF, PTEN tumor suppressor genes in human glioma cell lines. Brain Pathol., *9:* 469–479, 1999.
11. Haas-Kogan, D., Shalev, N., Wong, M., Mills, G., Yount, G., and Stokoe, D. Protein kinase B (PKB/Akt) activity is elevated in glioblastoma cells due to mutation of the tumor suppressor PTEN/MMAC. Curr. Biol., *8:* 1195–1198, 1998.
12. Gingras, A. C., Raught, B., and Sonenberg, N. Regulation of translation initiation by FRAP/mTOR. Genes Dev., *15:* 807–826, 2001.
13. Hashemolhosseini, S., Nagamine, Y., Morley, S. J., Desrivieres, S., Mercep, L., and Ferrari, S. Rapamycin inhibition of the G$_1$ to S transition is mediated by effects on cyclin D1 mRNA and protein stability. J. Biol. Chem., *273:* 14424–14429, 1998.
14. Luo, Y., Marx, S., Kiyokawa, H., Koff, A., Massague, J., and Marks, A. Rapamycin resistance tied to defective regulation of p27Kip1. Mol. Cell. Biol., *16:* 6744–6751, 1996.
15. Grewe, M., Gansauge, F., Schmid, R. M., Adler, G., and Seufferlein, T. Regulation of cell growth and cyclin D1 expression by the constitutively active FRAP-p70s6K pathway in human pancreatic cancer cells. Cancer Res., *59:* 3581–3587, 1999.
16. Sabatini, D. M., Erdjument-Bromage, H., Lui, M., Tempst, P., and Snyder, S. H. RAFT1: a mammalian protein that binds to FKBP12 in a rapamycin-dependent fashion and is homologous to yeast TORs. Cell, *78:* 35–43, 1994.
17. Brown, E. J., Albers, M. W., Shin, T. B., Ichikawa, K., Keith, C. T., Lane, W. S., and Schreiber, S. L. A mammalian protein targeted by G$_1$-arresting rapamycin-receptor complex. Nature (Lond.), *369:* 756–758, 1994.
18. Kahan, B. D., and Camardo, J. S. Rapamycin: clinical results and future opportunities. Transplantation, *72:* 1181–1193, 2001.
19. Withers, H. R., and Peters, L. J. Transmutability of dose and time. Commentary on the first report of RTOG 90003 (K. K. Fu *et al.*). Int. J. Radiat. Oncol. Biol. Phys., *48:* 1–2, 2000.
20. Fowler, J. F., and Harari, P. M. Confirmation of improved local-regional control with altered fractionation in head and neck cancer. Int. J. Radiat. Oncol. Biol. Phys., *48:* 3–6, 2000.
21. Jones, B., and Dale, R. G. Inclusion of molecular biotherapies with radical radiotherapy: modeling of combined modality treatment schedules. Int. J. Radiat. Oncol. Biol. Phys., *45:* 1025–1034, 1999.
22. Little, J. B., Hahn, G. M., Frindel, E., and Tubiana, M. Repair of potentially lethal radiation damage *in vitro* and *in vivo*. Radiology, *106:* 689–694, 1973.
23. Sarkaria, J., Gibson, D., Jordan, V., Fowler, J., Lindstrom, M., and Mulcahy, R. Tamoxifen induced increase in the potential doubling time (T_{pot}) of MCF-7 xenografts as determined by bromodeoxyuridine labeling and flow cytometry. Cancer Res., *53:* 4413–4417, 1993.
24. Hwang, H. S., Davis, T. W., Houghton, J. A., and Kinsella, T. J. Radiosensitivity of thymidylate synthase-deficient human tumor cells is affected by progression through the G$_1$ restriction point into S-phase: implications for fluoropyrimidine radiosensitization. Cancer Res., *60:* 92–100, 2000.
25. Hossi, H., Dilling, M. B., Shikata, T., Liu, L. N., Shu, L., Ashman, R. A., Germain, G. S., Abraham, R. T., and Houghton, P. J. Rapamycin causes poorly reversible inhibition of mTOR and induces p53-independent apoptosis in human rhabdomyosarcoma cells. Cancer Res., *59:* 886–894, 1999.
26. Sham, E., and Durand, R. E. Cell kinetics and repopulation mechanisms during multifraction irradiation of spheroids. Radiother. Oncol., *46:* 201–207, 1998.
27. Duchesne, G. M., and Peacock, J. H. Radiation cell survival and growth delay studies in multicellular spheroids of small-cell lung carcinoma. Int. J. Radiat. Biol. Phys. Chem. Med., *51:* 365–375, 1987.
28. Sutherland, R. M. Cell and environment interactions in tumor microregions: the multicell spheroid model. Science (Wash. DC), *240:* 177–184, 1988.
29. Meijer, L., Borgne, A., Mulner, O., Chong, J. P., Blow, J. J., Inagaki, N., Inagaki, M., Delcros, J. G., and Moulinoux, J. P. Biochemical and cellular effects of roscovitine, a potent and selective inhibitor of the cyclin-dependent kinases cdc2, cdk2 and cdk5. Eur. J. Biochem., *243:* 527–536, 1997.
30. Fowler, J. F., and Lindstrom, M. J. Loss of local control with prolongation in radiotherapy. Int. J. Radiat. Oncol. Biol. Phys., *23:* 457–467, 1992.
31. Sarkaria, J., Fowler, J., Lindstrom, M., Jordan, V., and Mulcahy, R. The decreased influence of overall treatment time on the response of human breast tumor xenografts following prolongation of the potential doubling time. Int. J. Radiat. Oncol. Biol. Phys., *31:* 833–840, 1995.
32. Harari, P. M., and Huang, S. M. Radiation response modification following molecular inhibition of epidermal growth factor receptor signaling. Semin. Radiat. Oncol. *11:* 281–289, 2001.
33. Rosenzweig, K. E., Youmell, M. B., Palayoor, S. T., and Price, B. D. Radiosensitization of human tumor cells by the phosphatidylinositol 3-kinase inhibitors wortmannin and LY294002 correlates with inhibition of DNA-dependent protein kinase and prolonged G$_2$/M delay. Clin. Cancer Res., *3:* 1149–1156, 1997.
34. Hardwick, J. S., Kuruvilla, F. G., Tong, J. K., Shamji, A. F., and Schreiber, S. L. Rapamycin-modulated transcription defines the subset of nutrient-sensitive signaling pathways directly controlled by the Tor proteins. Proc. Natl. Acad. Sci. USA, *96:* 14866–14870, 1999.
35. Guba, M., von Breitenbuch, P., Steinbauer, M., Koehl, G., Flegel, S., Homung, M., Bruns, C. J., Zuelke, C., Farkas, S., Anthuber, M., Jauch, K. W., and Geissler, E. K. Rapamycin inhibits primary and metastatic tumor growth by antiangiogenesis: involvement of vascular endothelial growth factor. Nat. Med., *8:* 128–135, 2002.
36. Zundel, W., Schindler, C., Haas-Kogan, D., Koong, A., Kaper, F., Chen, E., Gottschalk, A. R., Ryan, H. E., Johnson, R. S., Jefferson, A. B., Stokoe, D., and Giaccia, A. J. Loss of PTEN facilitates HIF-1-mediated gene expression. Genes Dev., *14:* 391–396, 2000.
37. Mazure, N. M., Chen, E. Y., Laderoute, K. R., and Giaccia, A. J. Induction of vascular endothelial growth factor by hypoxia is modulated by a phosphatidylinositol 3-kinase/Akt signaling pathway in Ha-ras-transformed cells through a hypoxia inducible factor-1 transcriptional element. Blood, *90:* 3322–3331, 1997.
38. Maity, A., Pore, N., Lee, J., Solomon, D., and O'Rourke, D. M. Epidermal growth factor receptor transcriptionally up-regulates vascular endothelial growth factor expression in human glioblastoma cells via a pathway involving phosphatidylinositol 3′-kinase and distinct from that induced by hypoxia. Cancer Res., *60:* 5879–5886, 2000.
39. Hess, C., Vuong, V., Hegyi, I., Riesterer, O., Wood, J., Fabbro, D., Glanzmann, C., Bodis, S., and Pruschy, M. Effect of VEGF receptor inhibitor PTK787/ZK222584 combined with ionizing radiation on endothelial cells and tumour growth. Br. J. Cancer, *85:* 2010–2016, 2001.
40. Gorski, D. H., Beckett, M. A., Jaskowiak, N. T., Calvin, D. P., Mauceri, H. J., Salloum, R. M., Seetharam, S., Koons, A., Hari, D. M., Kufe, D. W., and Weichselbaum, R. R. Blockade of the vascular endothelial growth factor stress response increases the antitumor effects of ionizing radiation. Cancer Res., *59:* 3374–3378, 1999.
41. Geng, L., Donnelly, E., McMahon, G., Lin, P. C., Sierra-Rivera, E., Oshinka, H., and Hallahan, D. E. Inhibition of vascular endothelial growth factor receptor signaling leads to reversal of tumor resistance to radiotherapy. Cancer Res., *61:* 2413–2419, 2001.
42. Ning, S., Laird, D., Cherrington, J. M., and Knox, S. J. The antiangiogenic agents SU5416 and SU6668 increase the antitumor effects of fractionated irradiation. Radiat. Res., *157:* 45–51, 2002.

Exhibit 3

BMC Cancer

BioMed Central

Research article

Retroviral expression of a kinase-defective IGF-I receptor suppresses growth and causes apoptosis of CHO and U87 cells in-vivo

B Lynn Seely[1], Goli Samimi[2] and Nicholas JG Webster*[1,2,3]

Address: [1]Department of Medicine, University of California, San Diego, La Jolla, CA 92093, USA, [2]UCSD Cancer Center, University of California, San Diego, La Jolla, CA 92093, USA and [3]Medical Research Service, San Diego Veterans Affairs Healthcare System, San Diego, CA 92161, USA

E-mail: B Lynn Seely - lseely@producthealth.com; Goli Samimi - gsamimi@ucsd.edu; Nicholas JG Webster* - nwebster@ucsd.edu

*Corresponding author

Published: 31 May 2002

BMC Cancer 2002, 2:15

Received: 18 April 2002

Accepted: 31 May 2002

This article is available from: http://www.biomedcentral.com/1471-2407/2/15

Abstract

Background: Phosphatidylinositol-3,4,5-triphosphate (PtdInsP3) signaling is elevated in many tumors due to loss of the tumor suppressor PTEN, and leads to constitutive activation of Akt, a kinase involved in cell survival. Reintroduction of PTEN in cells suppresses transformation and tumorigenicity. While this approach works in-vitro, it may prove difficult to achieve in-vivo. In this study, we investigated whether inhibition of growth factor signaling would have the same effect as re-expression of PTEN.

Methods: Dominant negative IGF-I receptors were expressed in CHO and U87 cells by retroviral infection. Cell proliferation, transformation and tumor formation in athymic nude mice were assessed.

Results: Inhibition of IGF-IR signaling in a CHO cell model system by expression of a kinase-defective IGF-IR impairs proliferation, transformation and tumor growth. Reduction in tumor growth is associated with an increase in apoptosis in-vivo. The dominant-negative IGF-IRs also prevented growth of U87 PTEN-negative glioblastoma cells when injected into nude mice. Injection of an IGF-IR blocking antibody αIR3 into mice harboring parental U87 tumors inhibits tumor growth and increases apoptosis.

Conclusion: Inhibition of an upstream growth factor signal prevents tumor growth of the U87 PTEN-deficient glioma to the same extent as re-introduction of PTEN. This result suggests that growth factor receptor inhibition may be an effective alternative therapy for PTEN-deficient tumors.

Background

Phosphatidylinositol-(3,4,5)-trisphosphate (PIP3) is one of the major intracellular second messengers regulating growth, metabolism and vesicular trafficking [for reviews see refs [1–3]]. The level of (PIP3) in the cell is determined by the balance of kinase and phosphatase activity. PI-3Kinase activity is acutely regulated and a number of isoforms have been cloned that are activated in response to various stimuli [4]. The major phosphatidylinositol-3-phosphate phosphatase in cells is the tumor suppressor

PTEN [5,6]. This protein has a tonic inhibitory effect on PI-3Kinase signaling by reversing the 3'-phosphorylation. PTEN is altered or deleted in many human cancers [7–10]. In-vitro, cells that are deficient in PTEN show elevated PI-3Kinase signaling [11]. Reintroduction of PTEN in a variety of cancer cells, including glioma, breast, bladder and ovarian cancer cells, causes G1 arrest, inhibits tumorigenesis, and promotes anoikis [12–14]. Mechanistically, Akt activity is decreased, cell motility is decreased, expression of two cyclin-dependent kinase inhibitors p27 and p21 is increased, cyclin D1 is down-regulated, Rb phosphorylation is inhibited, and signaling via Grb2/SOS is suppressed [11,15]. The link between PTEN and cell growth is underscored by genetic experiments in mice. PTEN knockout mice die in-utero due to extensive overgrowth of the cephalic and caudal regions [12,16]. PTEN +/- heterozygous mice have a predisposition to tumors in multiple tissues often with loss of the second allele [17,18]. In-vitro, PTEN-/- embryonic stem cells and fibroblasts display increased proliferation and decreased sensitivity to apoptosis.

The PI-3Kinase-dependent activation of Akt is thought to play a central role in the cell survival pathway in many cells [7,19,20]. Elevated Akt activity and protein is found in many PTEN-deficient cancer cells. Akt directly phosphorylates and inactivates the pro-apoptotic proteins ASK1, BAD, caspase 9 [21–24]. Akt also induces the expression of the anti-apoptotic Bcl-2 and c-FLIP proteins, and suppresses the cell cycle inhibitor $p27^{KIP}$[25–28]. This later effect is via the phosphorylation and inactivation of the forkhead family of transcription factors AFX, FKHR and FKHR-L1. Although it is often assumed that elevated Akt activity is responsible for the increased survival of cancer cells, Akt activity is not the only pathway that is essential for cell survival. The MAPK pathway can also protect cells from apoptosis, as can constitutive activation of Stat3 signaling [29,30].

The IGF-I Receptor is a member of the large family of tyrosine kinase growth factor receptors. Signaling by the IGF-IR has been studied in many different cell types and is important for proliferation, survival, motility, adhesion, transformation, tumor formation and metastasis [for reviews see refs [31,32]]. The receptor can directly phosphorylate the insulin receptor substrate 1 (IRS-1) and Shc proteins in the intact cell causing activation of PI-3Kinase and ras signaling [33]. More recently, it has been shown that the IGF-IR signals via the $G\beta\gamma$ subunits of the heterotrimeric Gi complex to stimulate PI-3Kinase and ras, and also activates the JAK/Stat pathway to cause phosphorylation of Stat3 [34,35].

What is the evidence for the involvement of IGF-IR signaling in proliferation and cancer? Elegant studies in knockout mice have delineated the contribution of IGF-I, IGF-II and the IGF-I receptor to fetal growth [for review see ref [36]]. Embryonic fibroblasts derived from IGF-IR knockout embryos (R-cells) do not grow in serum-free medium, despite supplementation with a wide variety of other growth factors, and grow more slowly in media containing serum than wild-type cells [for reviews see refs [37,38]]. Additionally, all phases of the cell cycle are prolonged in the null cells suggesting that the IGF-IR is required throughout the cell cycle. A functional IGF-I receptor is required for successful cell transformation. IGF-IR-/- cells are not transformed by overexpression of SV40 T antigen, activated *ras*, or EGF or PDGF receptors. Transformation appears to involve autocrine stimulation as IGF-I production and secretion is increased in normal cells following transformation by SV40 T antigen, but the null cells cannot respond to the IGF-I so do not transform.

Interfering with the IGF signaling system can inhibit the growth of cancer cells in-vitro and in-vivo. Treatment with antagonistic peptide analogs of IGF-I, antisense oligos, or an adenovirus expressing IGF-IR antisense cRNA, prevents proliferation of cells in monolayers, transformation, and growth in athymic nude mice. This includes multiple human tumor cell lines including glioblastoma, melanoma, ovarian carcinoma, prostatic carcinoma, and breast carcinomas). [for reviews see refs [31],[39–41]]. The IGF-IR appears to function in transformation both by preventing apoptosis through activation of Akt and by stimulating proliferation through the ras-MAPK cascade. IGF-I can prevent *c-myc*-induced apoptosis in rat-1 fibroblasts, and neuronal apoptosis due to serum-starvation. IGF-IR-/- cells can proliferate in monolayers in the presence of serum but undergo apoptosis when put in suspension and are more sensitive to chemotherapeutic reagents. There is also evidence implicating the IGF-IR in metastasis. IGF-I produces a chemotactic response in human melanoma cells and antisense to the IGF-IR mRNA prevents metastasis in the murine carcinoma cell H-59.

In this study, we wanted to determine if disruption of IGF-I signaling could prevent growth of a tumor cell lacking PTEN. Elevated PI-3Kinase can be normalized by reintroduction of PTEN to reduce PIP3 levels, but it has not been shown that this effect can also be achieved by disruption of an upstream signal that stimulates PI-3Kinase activity. We have previously demonstrated the overexpression and hormone-independent activation of the IGF-IR in primary breast cancers [42]. Similar overexpression of the IGF-IR and the ligands IGF-I and IGF-II have been seen in human gliomas and astrocytomas [43–46]. Because of the important role for the IGF-IR in cell survival, we investigated whether a dominant negative IGF-IR could inhibit growth of the U87 glioma. This glioma is deficient in PTEN and

shows constitutive activation of Akt, which can be inactivated by re-introduction of PTEN [47].

Materials and Methods

Materials and Cell Culture

Antiphosphotyrosine antibodies (pY20) were from BD-Transduction Labs (Lexington, KY). Matrigel was from Becton-Dickinson (Bedford, MA) Athymic nude mice were purchased from Charles River (Wilmington, MA). Enhanced chemiluminescence reagents were from Amersham (Piscataway, NJ). [^{3}H]-thymidine (20 Ci/mmol) was from Perkin-Elmer/NEN Life Sciences (Boston, MA). Unless noted, all other reagents were supplied by Sigma Chemical Co. (St. Louis, MO) or Fisher Scientific Co. (Springfield, NJ). CHO cells were maintained in Hams F12 with 25 mM glucose with 50 units/ml penicillin, 50 μg/ml streptomycin, and 10% FCS in a 10 % CO_2 environment. U87 glioma cells were maintained in MEM-Earle's medium with non-essential amino acids, 1 mM sodium pyruvate, 10% FCS, 2 mM Glutamax and gentamycin sulphate in a 10% CO2 environment.

Immunoblotting

Cells were serum starved for 16 h in 12-well plates, then stimulated with IGF-I (10 or 100 ng/ml) for 5 min at 37°C. The cells were washed with ice-cold phosphate-buffered saline and solubilized in 2 × SDS-sample buffer containing 2 mM sodium orthovanadate and 200 mM sodium fluoride. The proteins were denatured by boiling for 5 min, then were separated by electrophoresis on 7.5% SDS-PAGE, and transferred to PVDF membranes. The filter was blocked with 3% BSA in TBS with 0.1% Tween 20 (T-TBS) for 30 min and incubated with the anti-phosphotyrosine antibodies at a dilution of 1:1000. The filters were washed with T-TBS for 30 min and incubated with horseradish-peroxidase conjugated secondary antibodies, and tyrosine-phosphorylated proteins were visualized by enhanced chemiluminescence.

Measurement of thymidine incorporation

Cells were grown to 75% confluence in six-well cluster plates. The growth medium was replaced with serum-free Ham's F12 for 36 h. Cells were stimulated with IGF-I at the indicated concentrations for 18 h. Cells were pulsed with [^{3}H]-thymidine, 2 μCi/ml, for 1 h at 37°C. The cells were washed five times in PBS, solubilized, the DNA precipitated with 10% trichloroacetic acid at 4°C, and counted in an scintillation counter.

Production of pseudo-typed retrovirus

The wild-type IGF-IR cDNA or a mutant cDNA, which contained a methionine substitution for lysine 1003 in the ATP-binding site of the kinase domain, were cloned into the retroviral vector pLPONL [57]. The pseudo-typed viruses were generated and purified by the UCSD Viral Vector Core. The plasmids were co-transfected into 293 cells with an expression vector for the Vesicular Stomatitis Virus-G protein. This coat protein allows the virus to be concentrated and confers greater tropism. Cell culture supernatants and cells were harvested and the virus concentrated. Viruses were titered on NIH3T3 cells and the number of G418 resistant colonies counted. A control virus containing the E. coli β-galactosidase gene was obtained from the Viral Vector Core.

Growth in Soft Agar

Cells were trypsinized and 10^4 cells plated in 35 mm petri dishes in complete medium containing 0.35% agarose over a layer of 0.7% agarose in complete medium. Cells were allowed to grow for 14–21 days or until colonies were >125 μm in diameter. Fresh medium was layered above the agarose every 3–5 days. Colonies were stained with Crystal Violet and counted.

Tumor Growth in Athymic Nude Mice

Housing and all procedures using nude mice were approved by the animal care committee at UCSD. The cells for injection were trypsinized in sterile PBS, pelleted by centrifugation at 300 × g for 2 min. and washed twice in sterile saline. Cells were resuspended in 100 μl sterile saline and counted using a hemacytometer. The appropriate number of cells was diluted into 50 μl sterile saline and then added to an equal volume of sterile Matrigel on ice. This suspension was injected subcutaneously on the rear flank of athymic nude mice using a sterile syringe and 22-gauge needle. Mice were observed on a twice-weekly basis to check for tumor growth. Tumors were measured with calipers in three dimensions and tumor volume calculated assuming the tumors were ellipsoid. At the end of the study, the tumors were excised, measured, weighed, and then fixed in 10% formalin. Tumors were embedded in paraffin, sectioned and stained with hematoxylin-eosin or for apoptosis using the TUNEL assay (Roche, Indianapolis, IN).

Results and Discussion

Inhibition of the IGF-I receptor by expression of a kinase inactive mutant inhibits proliferation of Chinese hamster ovary (CHO) cells

Before embarking on studies in human tumor cells, we verified that our dominant negative approach would work in a model system. To inhibit the IGF-IR, we took advantage of the fact that the IGF-I receptor is a hetero-tetramer. Activation of the native receptor requires the trans-phosphorylation of two kinase domains [48]. Hence, expression of an excess of kinase-defective IGF-I receptors causes the formation of hybrid molecules containing one half an endogenous wild-type receptor and the other half a kinase-defective transfected receptor. These hybrids should be kinase inactive and signaling incompetent. Similar ap-

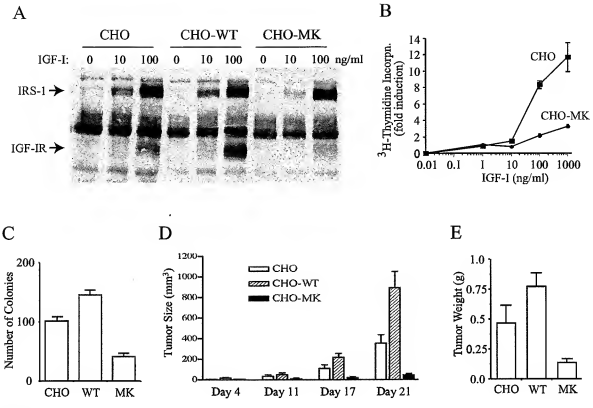

Figure 1

Expression of a kinase inactive IGF-IR impairs tumorigenesis. CHO cells express 5×10^4 IGF-IRs, CHO-WT cells express 2×10^5 wild-type IGF-IRs, and the CHO-MK cells express 2×10^5 mutant IGF-IRs that contain a Lysine to Methionine point mutation in the ATP-binding site (MK1003). Panel A: IGF-I stimulated whole cell tyrosine phosphorylation. Serum-starved cells were stimulated with IGF-I (10 or 100 ng/ml) for 5 min and whole cell extracts immunoblotted for phosphotyrosine. The positions of the β-subunit of the IGF-IR and IRS-1 are indicated. Panel B: Serum-starved CHO or CHO-MK cells were stimulated with increasing concentrations of IGF-I for 18 h then pulsed with ^{3}H-thymidine for 1 h. DNA was precipitated with TCA and counted. Panel C: ten thousand cells were plated in soft agar in complete medium for 14–21 days. Colonies > 125 μm in diameter were counted after staining with crystal violet. Panel D: ten million cells were injected subcutaneously into the rear flank of athymic nude mice. Tumor size was measured with calipers every few days. Graph shows mean tumor volume (± SEM) as a function of time. Panel E: Mice were euthanized after 21 days and the tumors excised, weighed and fixed for staining. Graph shows mean tumor weight (± SEM).

proaches have been used successfully in other studies [49–52].

Initially, we tested Chinese hamster ovary (CHO) cells that had been stably transfected with expression vectors for kinase-inactive or wild type IGF-I receptors [53]. The parental CHO cell line expresses ~50,000 endogenous IGF-IRs, the transfected wild-type (CHO-WT) cell line expresses ~250,000 IGF-IRs, and the kinase-defective (CHO-MK) cell line expresses ~250,000 mutant IGF-IRs. Thus, the transfected cells express the human IGF-IR at approximately five fold higher levels than the endogenous receptor. The mutant receptor contains a lysine to methionine (MK) point mutation at position 1003 in the ATP binding site of the kinase domain and has no measurable kinase activity. Two clonal lines expressing the MK receptor were used with identical results.

We assessed the ability of the IGF-IRs of each cell line to undergo autophosphorylation in response to increasing concentrations of IGF-I. Cells were stimulated with increasing concentrations of IGF-I, and whole cell lysates immunoblotted for tyrosine-phosphorylated proteins. As expected, autophosphorylation of the IGF-IRs was observed in the CHO and CHO-WT cells but very little was seen in two different clones of CHO-MK cells, indicating that the kinase-defective receptors inhibited the endogenous wild-type hamster receptors (Figure 1A). The inhi-

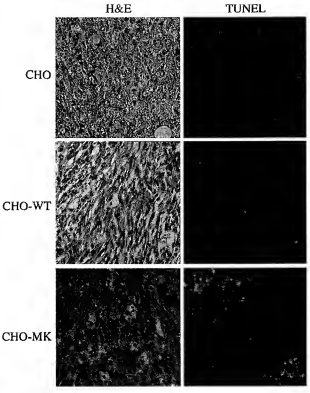

Figure 2
Staining of CHO cell tumors. Left panels: hematoxylin-eosin staining of sections of CHO (panel A), CHO-WT (panel B), and CHO-MK (panel C) tumors. Right panels: TUNEL staining for apoptotic cells. Apoptotic cells were detected with a fluorescein labeled secondary antibody and show green fluorescence.

bition was not complete however, as phosphorylation of IRS1, the major endogenous substrate in these cells, is still preserved at the higher dose of IGFI but inhibited at the lower dose. This is likely due to the level of receptor expression. The transfected receptors are expressed at four fold the level of the endogenous receptors. Assuming stochastic assembly of tetramers, 4% of receptors should be homodimers of signaling competent receptors that can phosphorylate IRS1. To confirm that the kinase-defective receptors were functioning in a dominant-negative fashion, we studied the ability of CHO and CHO-MK cells to incorporate ^{3}H-thymidine into DNA in response to IGF-I stimulation. Serum-starved cells were stimulated with increasing concentrations if IGF-I and then pulsed with ^{3}H-thymidine. The ability of the CHO-MK cells to incorporate thymidine in response to IGF-I is markedly diminished as compared to the parental cell line (Figure 1B).

We then tested colony formation in soft agar as an indicator of cellular transformation. Cells were trypsinized, counted and equivalent numbers of cells plated in soft agar in complete medium. Cells were cultured for 14 – 21 days and then the number of colonies counted. Overexpression of the wild-type IGF-IRs increased the number of colonies, and overexpressing the kinase-defective receptors reduced the number of colonies by 60% (Figure 1C). Not only did we observe a difference of the number of colonies, but CHO-MK colonies were smaller than either the parental CHO or CHO-WT colonies (data not shown).

We next studied the ability of each of these cell lines to form tumors in athymic nude mice. Ten million (10^{7}) cells from each cell line were injected subcutaneously into the flanks of five athymic nude mice. Tumor size was measured biweekly. The mice were euthanized at the end of three weeks and the tumors excised and weighed (Figure 1D & 1E). At this high level of innoculum, there was no difference in tumor incidence (data not shown). However, expression of the wild-type IGF-IR accelerated tumor growth and tumors were larger at sacrifice. The kinase defective IGF-IR, on the other hand, delayed the appearance of tumors and smaller tumors were found at sacrifice.

The tumors were imbedded in paraffin and sections were stained with hematoxylin and eosin (Figure 2, left panels). The sections were also stained for the presence of apoptosis using the TUNEL method. Apoptotic cells image as fluorescent green (Figure 2, right panels). The typical histology of CHO tumors is shown in panel A. Cells transfected with the wild-type IGF-IR have a more streaming morphology characteristic of human ovarian tumors (Panel B). Cells transfected with the kinase-defective IGF-IR showed a more benign morphology with no invasion of the capsule (Panel C and data not shown). Very few apoptotic cells are seen in the CHO parental and CHO-WT cells, whereas apoptotic cells are seen throughout the tumor from the kinase-defective CHO-MK cells. These results confirm that the kinase defective IGF-IR is able to inhibit tumor growth in a model system.

An inhibitory antibody to the IGF-IR inhibits growth of U87 tumors

Adenoviral expression of wild-type PTEN can inhibit U87 tumor growth indicating that elevated PI-3Kinase signaling is responsible for the increased proliferation and survival of these cells [47,54]. Our subsequent studies were designed to test whether interruption of an upstream growth factor signal would have the same growth inhibitory effect as reintroduction of PTEN. To test initially whether the PTEN-deficient U87 glioma cells might be susceptible to inhibition of the IGF-IR, we measured colony formation and tumor growth in the presence of an inhibitory antibody to the human IGF-IR (αIR3). This antibody prevents binding of IGF-I or IGF-II to the extracellular domain of the IGF-IR, and has been shown to pre-

vent the formation of MDA231 tumors in nude mice [55]. U87 cells were plated in soft agar in the presence of αIR3 or a control antibody. Cells were cultured for 14 days and the number of colonies counted. The presence of the inhibitory antibody reduced the number of colonies growing in soft agar but the control antibody had no effect (Table 1). U87 cells were then injected into nude mice as before. Mice received biweekly intraperitoneal injections of 100 μg of αIR3 or control antibody starting 3 days after injection of the cells. The αIR3 injections reduced the number of tumors by >60% (Table 1). The tumors were excised, fixed and stained for apoptosis. Tumors from mice treated with the αIR3 antibody showed extensive apoptosis unlike control tumors (Figure 3). These results confirm that inhibition of IGF-I signaling by an inhibitory antibody can suppress growth of a PTEN-deficient glioma cell line.

Table 1: Effect of antibody αIR3 on transformation and tumor growth.

	Untreated	αIR3	Mouse IgG
Colonies in soft agar	28 ± 3	11 ± 2	27 ± 2
Tumors in nude mice	-	4/16 (25%)	11/16 (69%)

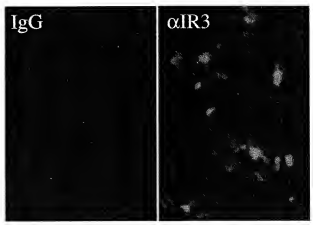

Figure 3
Treatment with an inhibitory antibody against the IGF-IR. One million U87 cells were injected subcutaneously into the rear flanks of athymic nude mice. Mice received intraperitoneal injections of 100 μg of αIR3 or control IgG every two days starting on the third day after inoculation with cells. Each group consisted of eight mice that each received two injections of cells. Tumors were excised, fixed, sectioned and stained for apoptosis using the TUNEL assay. Left panel shows tumor from mice treated with control IgG; right panel shows tumor from mice treated with αIR3. TUNEL positive cells show green fluorescence.

Retroviral expression of the kinase inactive IGF-I Receptor inhibits growth of U87 glioblastoma cells in-vivo

To make expression of kinase defective IGF-I receptors in different cell lines more tractable, we generated pseudotyped retroviruses expressing either the kinase-defective (MK) or wild-type (WT) IGF-I receptors. We also obtained a virus expressing the beta-galactosidase (LacZ) protein to measure infection efficiency and serve as a virus control. U87 cells were infected with the MK, WT or LacZ viruses and selected with G418. Pools of cells containing stably integrated retroviruses were then used in transformation and tumor growth experiments. Binding studies showed that the U87-LacZ cells express 10^5 endogenous IGF-IRs per cell, while the U87-WT and U87-MK cells express 3×10^6 and 2×10^6 receptors per cells respectively. Thus, the retrovirus allows 20 to 30-fold overexpression of the transfected receptor.

To test the function of the virally encoded receptors, we measured IGF-I stimulated autophosphorylation of the IGF-IR and phosphorylation of IRS-1. Phosphorylation IRS-1 was evident in the LacZ infected cells but little IGF-IR phosphorylation was seen as the cells express few receptors (Figure 4). Infection with the WT virus leads to a large increase in IGF-IR and IRS-1 tyrosine phosphorylation. Infection with the MK virus eliminated the IGF-I stimulated phosphorylation of IRS-1 confirming that the expressed receptor was acting as a dominant negative to inhibit the endogenous receptors. The dominant negative effect is much greater in these cells than the CHO cells (Figure 1) as the virus expresses the transfected receptors at a much higher level.

The three infected U87 glioma cells were then injected into nude mice. Eight to twelve mice were studied for each cell line and each mouse received two injections. In two different experiments, mice were inoculated with 10^6 or 5×10^5 cells. Tumors were excised after 6 or 10 weeks and weighed (Table 2). The WT-infected cells had the highest frequency of tumor formation and the MK-infected cells the lowest in both cases. WT-infected cells gave the largest tumors in both experiments demonstrating that overexpression of the IGF-IR in a malignant cell can enhance tumor formation as we observed for the CHO cells. The MK-infected cells gave fewer tumors in both experiments, but more importantly, those tumors that did form were much smaller. The results obtained with the dominant negative IGF-IR are identical to published results reintroducing PTEN, hence, inhibition of upstream PI-3Kinase signaling might be a useful approach for PTEN-deficient tumors.

The tumors were imbedded in paraffin and sections were stained with hematoxylin and eosin (Figure 5). The U87-

Table 2: Growth of infected U87 cells in nude mice.

	U87		U87-WT		U87-MK	
# cells[a]	#tumors (%)	Weight (g)	#tumors (%)	Weight (g)	#tumors (%)	Weight (g)
5×10^5	4/14 (29%)	0.48 ± 0.11	11/16 (69%)	0.67 ± 0.15	2/14 (14%)	0.13* ± 0.02
10^6	16/24 (67%)	0.43 ± 0.13	16/18 (89%)	0.57 ± 0.1	11/24 (46%)	0.12* ± 0.02

Weight is given as mean ± SEM. (a) mice with 5×10^5 cells sacrificed after 10 weeks, mice with 10^6 cells sacrificed after 6 weeks. Asterisks denote statistical significance ($P < 0.05$) versus parental cells

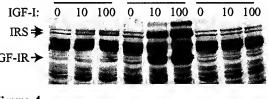

Figure 4
Retroviral expression of wild-type and mutant IGF-IRs in U87 glioma cells. U87 cells stably infected with pseudotyped retroviruses expressing β-galactosidase (LacZ), wild-type IGF-IR (WT) or kinase defective IGF-IR (MK) were rendered quiescent by serum-starvation then stimulated with IGF-I (10 or 100 ng/ml) for 5 min. Whole cell extracts were immunoblotted for phosphotyrosine. The positions of the β-subunit of the IGF-IR and the IRS proteins are indicated.

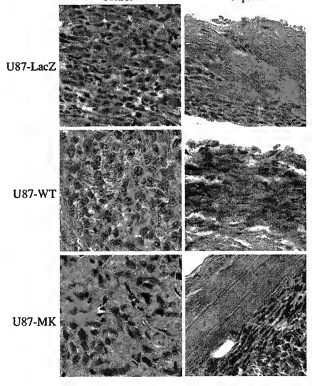

Figure 5
Staining of U87 tumors. Tumors were fixed, sectioned and stained with hematoxylin-eosin. Left panels: staining of central tumor section. Right panels: staining of tumor capsule. White arrows indicate infiltration of tumor cells into the capsule. Tumors from U87-LacZ cells are shown in the top panels, tumors from U87-WT cells (wild-type IGF-IR) in the middle panels, and tumors from U87-MK cells (kinase defective IGF-IR) in the bottom panels.

LacZ tumors are very cellular with small regular nuclei (left panel) and show some invasion of the capsule by tumor cells (right panel). The tumors from U87 cells infected with the IGF-IR virus are also very cellular, but the cells have larger nuclei (left panel) and have completely invaded the capsule (right panel). The tumors from U87 cells infected with the kinase inactive IGF-IR are less cellular with larger areas of stroma (left panel). Numerous irregular nuclei are apparent. There is no invasion of the capsule by tumor cells (right panel). The irregular nuclei and intact capsule are consistent with data from other cells showing that inhibition of IGF-IR expression causes apoptosis and prevents metastasis.

The idea that the IGF-IR might be a valuable target for the treatment of brain tumors is supported by a recent pilot study in twelve patients with malignant astrocytomas [56]. All patients had grade 3 or 4 astrocytomas and had failed on standard therapy. The PTEN status of their primary tumors was not known. After surgery, autologous glioma cells were collected and treated ex-vivo with IGF-IR antisense oligos and re-implanted in diffusion cham-

bers for 24 h. Clinical and radiological improvements were seen in eight of the twelve patients. Five patients showed a lymphocytic infiltration after antisense treatment indicating that knocking out the IGF-IR induced an immune response. It would be interesting to determine whether response to this treatment correlated with loss of PTEN in the primary tumors.

Conclusions

Loss of PTEN is a very common occurrence in human tumors. Restoring PTEN protein or function to reduce PI-3Kinase signaling prevents tumor growth in animal models. However, it may not be possible to restore PTEN in human tumors. Direct inhibition of PI-3Kinase activity may not be feasible either as it is likely to have severe side effects. Our results suggest that a therapeutic strategy to inhibit the upstream stimulus for PI-3Kinase through blockade of growth factor receptors may provide a workable alternative.

Abbreviations

PIP3: Phosphatidyl-3,4,5-triphosphate; DMEM: Dulbecco's Modified Eagle's Medium; PI-3Kinase: phosphatidylinositol-3-kinase; MAPK: mitogen-activated protein kinase; IGF: insulin-like growth factor; PTEN: phosphatase and tensin homolog deleted from chromosome 10; SOS: son-of-sevenless ras exchange factor; ASK: apoptosis stimulating kinase; FKHR: forkhead related protein; cFLIP: cellular FLICE interacting protein; BSA: bovine serum albumin; TBS: tris buffered saline; PVDF: polyvinylidene difluoride

Competing Interests

None declared.

Author Contributions

B.L.S. conducted the studies on CHO cells and the inhibitory antibody studies on U87 cells. G.S. performed the tumor growth studies with the U87 cells. N.J.G.W. constructed the pseudotyped retroviruses and drafted the manuscript.

Acknowledgements

This research was supported by a NIH Clinical Investigator Award (to B.L.S.) and a CapCURE award (to N.J.G.W.). We would like to acknowledge the expert technical assistance of Donna Reichart. N.J.G.W. is a faculty member of the UCSD Biomedical Sciences Graduate Program. B.L.S. current address is ProDuct Health Inc., Menlo Park, CA.

References

1. Rameh LE, Cantley LC: **The role of phosphoinositide 3-kinase lipid products in cell function.** *J Biol Chem* 1999, **274**:8347-8350
2. Katso R, Okkenhaug K, Ahmadi K, White S, Timms J, Waterfield MD: **Cellular function of phosphoinositide 3-kinases: implications for development, homeostasis, and cancer.** *Annu Rev Cell Dev Biol* 2001, **17**:615-675
3. Cantrell DA: **Phosphoinositide 3-kinase signalling pathways.** *J Cell Sci* 2001, **114**:1439-1445
4. Vanhaesebroeck B, Waterfield MD: **Signaling by distinct classes of phosphoinositide 3-kinases.** *Exp Cell Res* 1999, **253**:239-254
5. Leslie NR, Downes CP: **PTEN: The down side of PI 3-kinase signalling.** *Cellular Signalling* 2002, **14**:285-295
6. Maehama T, Dixon JE: **PTEN: a tumour suppressor that functions as a phospholipid phosphatase.** *Trends Cell Biol* 1999, **9**:125-128
7. Cantley LC, Neel BG: **New insights into tumor suppression: PTEN suppresses tumor formation by restraining the phosphoinositide 3-kinase/AKT pathway.** *Proc Natl Acad Sci U S A* 1999, **96**:4240-4245
8. Liaw D, Marsh DJ, Li J, Dahia PL, Wang SI, Zheng Z, *et al*: **Germline mutations of the PTEN gene in Cowden disease, an inherited breast and thyroid cancer syndrome.** *Nat Genet* 1997, **16**:64-67
9. Ali IU, Schriml LM, Dean M: **Mutational spectra of PTEN/MMAC1 gene: a tumor suppressor with lipid phosphatase activity.** *J Natl Cancer Inst* 1999, **91**:1922-1932
10. Dahia PL: **PTEN, a unique tumor suppressor gene.** *Endocr Relat Cancer* 2000, **7**:115-129
11. Davies MA, Koul D, Dhesi H, Berman R, McDonnell TJ, McConkey D, *et al*: **Regulation of Akt/PKB activity, cellular growth, and apoptosis in prostate carcinoma cells by MMAC/PTEN.** *Cancer Res* 1999, **59**:2551-2556
12. Di Cristofano A, Pandolfi PP: **The multiple roles of PTEN in tumor suppression.** *Cell* 2000, **100**:387-390
13. Yamada KM, Araki M: **Tumor suppressor PTEN: modulator of cell signaling, growth, migration and apoptosis.** *J Cell Sci* 2001, **114**:2375-2382
14. Teng DH, Hu R, Lin H, Davis T, Iliev D, Frye C, *et al*: **MMAC1/PTEN mutations in primary tumor specimens and tumor cell lines.** *Cancer Res* 1997, **57**:5221-5225
15. Ramaswamy S, Nakamura N, Vazquez F, Batt DB, Perera S, Roberts TM, *et al*: **Regulation of G1 progression by the PTEN tumor suppressor protein is linked to inhibition of the phosphatidylinositol 3-kinase/Akt pathway.** *Proc Natl Acad Sci U S A* 1999, **96**:2110-2115
16. Suzuki A, de la Pompa JL, Stambolic V, Elia AJ, Sasaki T, del Barco Barrantes I, *et al*: **High cancer susceptibility and embryonic lethality associated with mutation of the PTEN tumor suppressor gene in mice.** *Curr Biol* 1998, **8**:1169-1178
17. Stambolic V, Tsao MS, Macpherson D, Suzuki A, Chapman WB, Mak TW: **High incidence of breast and endometrial neoplasia resembling human Cowden syndrome in pten+/- mice.** *Cancer Res* 2000, **60**:3605-3611
18. Podsypanina K, Ellenson LH, Nemes A, Gu J, Tamura M, Yamada KM, *et al*: **Mutation of Pten/Mmac1 in mice causes neoplasia in multiple organ systems.** *Proc Natl Acad Sci U S A* 1999, **96**:1563-1568
19. Testa JR, Bellacosa A: **AKT plays a central role in tumorigenesis.** *PNAS* 2001, **98**:10983-10985
20. Datta SR, Brunet A, Greenberg ME: **Cellular survival: a play in three Akts.** *Genes Dev* 1999, **13**:2905-2927
21. Datta SR, Dudek H, Tao X, Masters S, Fu H, Gotoh Y, *et al*: **Akt phosphorylation of BAD couples survival signals to the cell-intrinsic death machinery.** *Cell* 1997, **91**:231-241
22. del Peso L, Gonzalez-Garcia M, Page C, Herrera R, Nunez G: **Interleukin-3-induced phosphorylation of BAD through the protein kinase Akt.** *Science* 1997, **278**:687-689
23. Kim AH, Khursigara G, Sun X, Franke TF, Chao MV: **Akt phosphorylates and negatively regulates apoptosis signal-regulating kinase 1.** *Mol Cell Biol* 2001, **21**:893-901
24. Cardone MH, Roy N, Stennicke HR, Salvesen GS, Franke TF, Stanbridge E, *et al*: **Regulation of cell death protease caspase-9 by phosphorylation.** *Science* 1998, **282**:1318-1321
25. Cheney IW, Neuteboom ST, Vaillancourt MT, Ramachandra M, Bookstein R: **Adenovirus-mediated gene transfer of MMAC1/PTEN to glioblastoma cells inhibits S phase entry by the recruitment of p27Kip1 into cyclin E/CDK2 complexes.** *Cancer Res* 1999, **59**:2318-2323
26. Weng LP, Brown JL, Eng C: **PTEN coordinates G(1) arrest by down-regulating cyclin D1 via its protein phosphatase activity and up-regulating p27 via its lipid phosphatase activity in a breast cancer model.** *Hum Mol Genet* 2001, **10**:599-604
27. Winter RN, Kramer A, Borkowski A, Kyprianou N: **Loss of Caspase-1 and Caspase-3 Protein Expression in Human Prostate Cancer.** *Cancer Res* 2001, **61**:1227-1232

28. Pugazhenthi S, Nesterova A, Sable C, Heidenreich KA, Boxer LM, Heasley LE, *et al*: **Akt/protein kinase B up-regulates Bcl-2 expression through cAMP-response element-binding protein.** *J Biol Chem* 2000, **275**:10761-10766
29. Scrimgeour AG, Blakesley VA, Stannard BS, LeRoith D: **Mitogen-activated protein kinase and phosphatidylinositol 3-kinase pathways are not sufficient for insulin-like growth factor I-induced mitogenesis and tumorigenesis.** *Endocrinology* 1997, **138**:2552-2558
30. Ni Z, Lou W, Leman ES, Gao AC: **Inhibition of Constitutively Activated Stat3 Signaling Pathway Suppresses Growth of Prostate Cancer Cells.** *Cancer Res* 2000, **60**:1225-1228
31. Baserga R: **The IGF-I receptor in cancer research.** *Exp Cell Res* 1999, **253**:1-6
32. LeRoith D, Baserga R, Helman L, Roberts CT: **Insulin-like growth factors and cancer.** *Ann Intern Med* 1995, **122**:54-59
33. LeRoith D, Werner H, Beitner-Johnson D, Roberts CTJ: **Molecular and cellular aspects of the insulin-like growth factor I receptor.** *Endocr. Rev.* 1995, **16**:143-163
34. Luttrell LM, Van Biesen T, Hawes BE, Koch WJ, Touhara K, Lefkowitz RJ: **G beta gamma subunits mediate mitogen-activated protein kinase activation by the tyrosine kinase insulin-like growth factor 1 receptor.** *J. Biol. Chem.* 1995, **270**:16495-16498
35. Zong CS, Zeng L, Jiang Y, Sadowski HB, Wang LH: **Stat3 plays an important role in oncogenic Ros- and insulin-like growth factor I receptor-induced anchorage-independent growth.** *J Biol Chem* 1998, **273**:28065-28072
36. Accili D, Nakae J, Kim JJ, Park BC, Rother KI: **Targeted gene mutations define the roles of insulin and IGF-1 receptors in mouse embryonic development.** *J Pediatr Endocrinol Metab* 1999, **12**:475-485
37. Baserga R: **The insulin-like growth factor I receptor: a key to tumor growth?** *Cancer Res.* 1995, **55**:249-252
38. Baserga R, Hongo A, Rubini M, Prisco M, Valentinis B: **The IGF-I receptor in cell growth, transformation and apoptosis.** *Biochim Biophys Acta* 1997, **1332**:F105-126
39. Baserga R, Resnicoff M, Dews M: **The IGF-I receptor and cancer.** *Endocrine* 1997, **7**:99-102
40. Pollak M, Beamer W, Zhang JC: **Insulin-like growth factors and prostate cancer.** *Cancer Metastasis Rev* 1999, **17**:1998-383
41. Yee D: **The insulin-like growth factor system as a target in breast cancer.** *Breast Cancer Res. Treat.* 1994, **32**:85-95
42. Resnik JL, Reichart DB, Huey K, Webster NJ, Seely BL: **Elevated insulin-like growth factor I receptor autophosphorylation and kinase activity in human breast cancer.** *Cancer Res* 1998, **58**:1159-1164
43. Ogino S, Kubo S, Abdul-Karim FW, Cohen ML: **Comparative immunohistochemical study of insulin-like growth factor II and insulin-like growth factor receptor type I in pediatric brain tumors.** *Pediatr Dev Pathol* 2001, **4**:23-31
44. Antoniades HN, Galanopoulos T, Neville-Golden J, Maxwell M: **Expression of insulin-like growth factors I and II and their receptor mRNAs in primary human astrocytomas and meningiomas; In vivo studies using in situ hybridization and immunocytochemistry.** *Int J Cancer* 1992, **50**:215-222
45. Gammeltoft S, Ballotti R, Nielsen FC, Kowalski A, Van Obberghen E: **Receptors for insulin-like growth factors in the central nervous system: structure and function.** *Horm Metab Res* 1988, **20**:436-442
46. Sandberg AC, Engberg C, Lake M, von Holst H, Sara VR: **The expression of insulin-like growth factor I and insulin-like growth factor II genes in the human fetal and adult brain and in glioma.** *Neurosci Lett* 1988, **93**:114-119
47. Wick W, Furnari FB, Naumann U, Cavenee WK, Weller M: **PTEN gene transfer in human malignant glioma: sensitization to irradiation and CD95L-induced apoptosis.** *Oncogene* 1999, **18**:3936-3943
48. Lammers R, Van Obberghen E, Ballotti R, Schlessinger J, Ullrich A: **Transphosphorylation as a possible mechanism for insulin and epidermal growth factor receptor activation.** *J. Biol. Chem.* 1990, **265**:16886-16890
49. Treadway JL, Morrison BD, Soos MA, Siddle K, Olefsky J, Ullrich A, *et al*: **Transdominant inhibition of tyrosine kinase activity in mutant insulin/insulin-like growth factor I hybrid receptors.** *Proc. Natl. Acad. Sci. U.S.A.* 1991, **88**:214-218
50. Seely BL, Reichart DR, Takata Y, Yip C, Olefsky JM: **A functional assessment of insulin/insulin-like growth factor-I hybrid receptors.** *Endocrinology* 1995, **136**:1635-1641
51. Kalebic T, Blakesley V, Slade C, Plasschaert S, Leroith D, Helman LJ: **Expression of a kinase-deficient IGF-I-R suppresses tumorigenicity of rhabdomyosarcoma cells constitutively expressing a wild type IGF-I-R.** *Int J Cancer* 1998, **76**:223-227
52. Burgaud JL, Resnicoff M, Baserga R: **Mutant IGF-I receptors as dominant negatives for growth and transformation.** *Biochem. Biophys. Res. Commun.* 1995, **214**:475-481
53. Hsu D, Knudson PE, Zapf A, Rolband GC, Olefsky JM: **NPXY motif in the insulin-like growth factor-I receptor is required for efficient ligand-mediated receptor internalization and biological signaling.** *Endocrinology* 1994, **134**:744-750
54. Cheney IW, Johnson DE, Vaillancourt MT, Avanzini J, Morimoto A, Demers GW, *et al*: **Suppression of tumorigenicity of glioblastoma cells by adenovirus-mediated MMAC1/PTEN gene transfer.** *Cancer Res* 1998, **58**:2331-2334
55. Arteaga CL, Kitten LJ, Coronado EB, Jacobs S, Kull FC, Allred DG, *et al*: **Blockade of the type I somatomedin receptor inhibits growth of human breast cancer cells in athymic mice.** *J Clin Invest* 1989, **84**:1418-1423
56. Andrews DW, Resnicoff M, Flanders AE, Kanyon L, Curtis M, Merli G, *et al*: **Results of a Pilot Study Involving the Use of an Antisense Oligodeoxynucleotide Directed Against the Insulin-Like Growth Factor Type I Receptor in Malignant Astrocytomas.** *J Clin Oncol* 2001, **19**:2189-2200
57. Friedmann T, Yee JK: **Pseudotyped retroviral vectors for studies of human gene therapy.** *Nat. Med.* 1995, **1**:275-277

Pre-publication history

The pre-publication history for this paper can be accessed here:

http://www.biomedcentral.com/1471-2407/2/15/prepub

Exhibit 4

0021-972X/93/7706-1388$03.00/0
Journal of Clinical Endocrinology and Metabolism

Vol. 77, No. 5
Printed in U.S.A.

Inhibition of Growth of the Human Malignant Glioma Cell Line (U87MG) by the Steroid Hormone Antagonist RU486*

JACEK PINSKI, GABOR HALMOS, YUTAKA SHIRAHIGE, JAMES L. WITTLIFF, AND ANDREW V. SCHALLY

Endocrine, Polypeptide and Cancer Institute, Veterans Administration Medical Center (J.P., G.H., Y.S., A.V.S.), and Section of Experimental Medicine, Tulane University School of Medicine (J.P., G.H., Y.S., A.V.S.), New Orleans, Louisiana 70146; and the Hormone Receptor Laboratory, University of Louisville (J.L.W.), Louisville, Kentucky 40292

ABSTRACT

Treatment of nude mice bearing xenografts of the human malignant glioma U87MG cell line with the steroid hormone antagonist RU486 for 4 weeks resulted in a significant and dose-dependent suppression of tumor volume and weight. Receptor analyses of tumor cytosol preparations demonstrated a single class of high affinity binding sites for dexamethasone, but the absence of receptors for progesterone. RU486 also nullified the stimulatory effect of dexamethasone on proliferation of U87MG cells *in vitro*. These results indicate that the growth of U87MG human malignant glioma is dependent on corticoids. The antiproliferative effect of RU486 appears to be due to the inhibition of binding of glucocorticoid hormones to their receptor proteins. Our results suggest a new therapy for some brain tumors, such as malignant gliomas based on the steroid hormone antagonist RU486. (*J Clin Endocrinol Metab* **77:** 1388–1392, 1993)

APPROXIMATELY 17,000 new cases of brain tumors were reported in the U.S. in 1992. Brain tumors are responsible for about 12,000 deaths annually in the U.S. (1). Certain brain tumors, such as malignant astrocytoma or glioblastoma, also known as malignant glioma or astrocytoma grade 3, are associated with very low survival rates (1, 2). Surgery, radiation, and chemotherapy are of limited effectiveness in the treatment of malignant gliomas, and other therapeutic approaches must be explored.

Steroid hormone receptors have been detected in benign brain tumors, such as meningiomas, and in various malignant brain tumors, including malignant gliomas (3–8), suggesting that some of these tumors might be hormone dependent. Glucocorticoid receptors (GR) have been demonstrated in malignant glioma specimens (3–5). Survival and proliferation of cell cultures from human malignant gliomas are enhanced by the addition of pharmacological doses of glucocorticoids (4, 9, 10). On the basis of the frequent detection of sex steroid receptors, especially those for progesterone in meningiomas (6, 11, 12), the steroid hormone antagonist RU486 is being used in clinical trials for the treatment of this tumor (13, 14). The steroid RU486 has potent antiprogestin and antiglucocorticoid properties (15) and has high affinity for both human progesterone and GR (*i.e.* K_d values of 10^{-9}–10^{-10} mol/L), but is devoid of significant agonistic effects on target cells (15). Antagonistic properties of RU486 for progesterone and glucocorticoids have been demonstrated in different systems *in vivo* and *in vitro* (15). The applications for RU486 include contraception, medical abortion, and treatment of different forms of Cushing's syndrome (15).

In view of the potential involvement of steroid hormones, especially glucocorticoid-like hormones, in tumorigenesis of malignant glioma, we investigated the influence of RU486 on the growth of the human malignant glioma cell line U87MG in nude mice. In addition, cell growth studies were performed *in vitro* to determine whether RU486 has an inhibitory effect on dexamethasone-stimulated U87MG cells.

Materials and Methods

In vivo experiment

The U87MG malignant glioma cell line obtained from American Type Culture Collection (Rockville, MD) was grown as a monolayer in Basal Eagle's Medium supplemented with 10% fetal bovine serum, sodium pyruvate, and antibiotics and antimycotics. Cultures were incubated in 5% CO_2 in air at 37 C. Xenografts were initiated by sc injection of 1×10^7 cells into the left flank of 5 NCr nu/nu nude mice (received from NIH, Bethesda, MD). The tumors resulting after 4 weeks were transplanted sc by trocar needle into 40 male animals under methoxyflurane (Metofane) anesthesia. RU-486 (Mifepristone) was dissolved in 30% propylene glycol in water. The treatment was started 1 week after tumor transplantation, when the tumors measured approximately 40 mm^3, and continued for 4 weeks. The mice were divided into 3 groups (10/group); the control group was injected with distilled water containing 30% propylene glycol, group 2 with RU486 administered by daily sc injections at a dose of 0.1 mg/day·animal, and group 3 with RU486 at a dose of 0.5 mg/day·animal. The tumors were measured once a week for 4 weeks. Tumor volume was calculated as (length × width × height × 0.5236). Statistical significance was calculated by Duncan's new multiple range test (16).

Received March 8, 1993. Accepted July 27, 1993.

Address all correspondence and requests for reprints to: Dr. Andrew V. Schally, Veterans Administration Medical Center, 1601 Perdido Street, New Orleans, Louisiana 70146.

* This work was supported by the Medical Research Service of the V.A. (to A.V.S.).

Receptor assays

Epidermal growth factor (EGF) receptor levels were measured with membrane preparations of tumor samples using iodinated EGF and a RRA, as described previously (17). GR in cytosol fractions were characterized by RRA using [^{3}H]dexamethasone. This method is described in detail by Halmos *et al.* (18). Progesterone and estradiol receptors were measured by enzyme immunoassay method, as described by Pasic *et al.* (19).

In vitro experiment

Cells from 70–80% confluent cultures were seeded into Costar 24-multiwell plates (Costar, Cambridge, MA) at a density of 5×10^3 cells/well and grown in Eagle's Minimum Essential Medium supplemented with 1 mmol/L sodium pyruvate and 5% fetal bovine serum pretreated with dextran-coated charcoal. After 48 h (day 0), media were replaced with fresh media containing dexamethasone and/or RU486. The cell number for each well was determined in a Coulter counter after detachment of the cells by trypsinization on day 4. The cell viability, measured by trypan blue dye exclusion, was more than 90%.

Results and Discussion

To determine whether the growth *in vivo* of human malignant glioma may be inhibited by antisteroid RU486, nude mice bearing xenografts of the U87MG glioma cell line were treated with various doses of RU486. Tumor growth in animals given RU486 at a dose of 0.1 mg/day was significantly ($P < 0.01$) inhibited within 3 weeks (Fig. 1). After 4 weeks, both tumor volume and tumor weight in the group receiving RU486 at a dose of 0.1 mg were significantly reduced to 1246.4 ± 236.9 mm^3 and 1.8 ± 0.2 g compared to the control groups (2399.0 ± 360.8 mm^3 and 2.9 ± 0.5 g, respectively; Table 1). Therapy with the higher dose of RU486 (0.5 mg/day) was even more effective, resulting in a greater reduction in tumor volume, which was statistically significant after only 1 week of treatment (Fig. 1). Tumor volume was significantly reduced ($P < 0.01$) in the group treated with RU486 at a dose of 0.5 mg to 616.5 ± 143.1 mm^3 at the termination of the experiment. Tumor weight also was decreased to 0.6 ± 0.1 g (Table 1). In animals treated

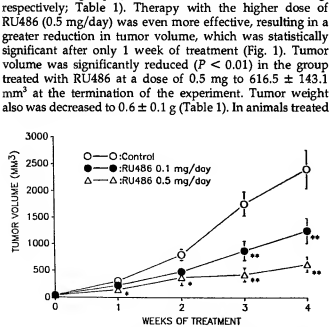

FIG. 1. Influence of RU486 treatment on tumor volume in male nude mice bearing U87MG human malignant gliomas. The mice were treated with the antagonist RU486 in doses of 0.1 and 0.5 mg/day, administered sc by daily injections. Statistical significance was calculated by Duncan's new multiple range test (16). *Vertical bars* represent the SEM. *, $P < 0.05$; **, $P < 0.01$ (*vs.* controls).

with 0.5 mg RU486, tumor doubling time was significantly increased ($P < 0.01$) to 8.3 ± 1.1 days compared to that in the control group, which had a doubling time of 4.9 ± 0.1 days (Table 1). The observations that RU486 inhibited the growth of meningiomas in patients (13, 14) suggest that RU486 crosses the blood-brain tumor barrier.

We next investigated steroid receptors, because the inhibitory effect of RU486 on tumor growth of U87MG xenografts could be produced by occupancy and blockade of steroid receptors. On the basis of our results of receptor analyses using a sensitive radioligand binding method, the presence of a single class of high affinity binding sites for dexamethasone was detected with a K_d of 3.6 ± 1.1 nmol/L (Fig. 2). The specific binding capacity was 159.7 ± 19.2 fmol/mg protein. The specific binding of RU486 was demonstrated by dose-dependent competition between [^{3}H]dexamethasone and RU486 for the GR (Fig. 3). Neither progesterone receptor (<3 fmol/mg protein) nor estrogen receptor (<7 fmol/mg protein) was detected in significant quantities (Table 2). Collectively, these results suggest that the tumor growth inhibitory effect of RU486 is mediated through a mechanism involving GR. RU486 has a high affinity for progesterone and GR, but exhibits little affinity for androgen and estrogen receptors (15). Our observations are in accordance with results obtained from biopsies of human malignant gliomas, which frequently contain GR (3, 4), but rarely exhibit progesterone receptors, and then only at low concentrations (4, 5, 20).

Treatment of animals bearing U87MG glioblastoma with RU486 produced a marked decrease in the cytosolic concentration of GR (Table 2). This finding may be due to the binding of the RU486-GR complexes to DNA in cell nuclei as a result of translocation (21). The apparent dissociation constants (K_d) of the glucocorticoid-binding sites were similar in all tissue samples from both groups (control and RU486-treated groups) and ranged between 1–7 nmol/L.

The lack of agonistic activity of RU486 has been suggested to be due to conformational alteration in the ligand-binding domain of the GR, which does not enhance transcriptional activity (22). RU486 may also down-regulate the GR concentration. Treatment of transfected COS-1 cells with RU486 previously was shown to down-regulate human GR mRNA (23). Another study suggested that progesterone enhanced EGF-induced growth of the feline mammary adenocarcinoma cell line K12 by increasing the number of functional EGF receptors (24). In our experiments, no significant differences were detected in either the concentration of EGF receptors or the binding affinity for EGF between control and RU486-treated tumors (Table 2). Receptors for EGF and insulin-like growth factor-I are known to be present in various brain tumors (25).

To establish that the growth of glioblastomas could be stimulated by glucocorticoids and blocked by RU486 *in vitro*, dexamethasone was added to the culture medium of U87MG cells in doses ranging from 10^{-11}–10^{-5} mol/L in the presence of 5% dextran-coated charcoal-treated fetal bovine serum (Fig. 4). Dexamethasone in the range of 10^{-5}–10^{-8} mol/L stimulated the growth of U87MG cells, and the maximal

TABLE 1. Influence of treatment with RU486 on tumor volume, body and tumor weights, tumor doubling time, and tumor specific growth delay time in nude mice with xenografts of the human malignant glioma cell line U87MG

Treatment group	Tumor vol (mm^3)		BW (g)	Tumor wt (g)	Tumor doubling time (days)	Specific growth delay time (days)
	Initial	Final at 4 weeks				
Control	43.0 ± 4.3	2399.0 ± 360.8	27.1 ± 0.6	2.9 ± 0.5	4.9 ± 0.1	
RU486 (0.1 mg day/animal)	43.6 ± 5.4	1246.4 ± 236.9[a]	26.3 ± 0.5	1.8 ± 0.2[b]	5.7 ± 0.3	0.16
RU486 (0.5 mg day/animal)	40.0 ± 4.9	616.5 ± 143.1[a]	25.6 ± 0.4	0.6 ± 0.1[a]	8.3 ± 1.1[a]	0.7

Values are the mean ± SEM. Significance was calculated by Duncan's multiple range test.
[a] $P < 0.01$ *vs.* controls.
[b] $P < 0.05$ *vs.* controls.

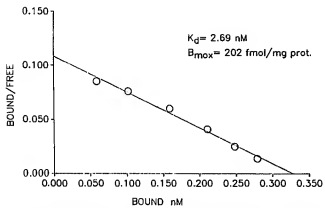

FIG. 2. Representative example of the Scatchard plots of [^{3}H]dexamethasone binding to the cytosolic fraction isolated from U87MG glioblastoma. Aliquots of cytosol were incubated with several concentrations (0.6–20 nmol/L) of [^{3}H]dexamethasone in the presence (nonspecific binding) or absence (total binding) of a 400-fold excess of nonlabeled dexamethasone for 18 h at 4 C. Six experiments were carried out, and in every experiment each concentration of radioligand was examined in duplicate.

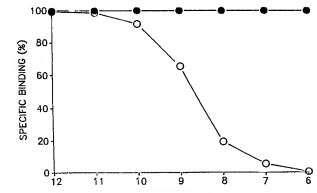

FIG. 3. Displacement of [^{3}H]dexamethasone (5 nmol/L) by varying concentrations (10^{-5}–10^{-12} mol/L) of RU486 (○) and other steroids (17β-estradiol, testosterone, and 5α-dihydrotestosterone; ●). 100% binding is defined as [^{3}H]dexamethasone binding in the absence of a competitor. Each *data point* represents the mean of at least three experiments, each performed in duplicate.

increase in cell numbers reached 91% at 10^{-5} mol/L dexamethasone. The growth stimulatory effect of 10^{-6} mol/L dexamethasone was significantly ($P < 0.01$) diminished in the presence of RU486 at concentrations of 10^{-6} and 10^{-5} mol/L (Fig. 4). At the 10^{-5} mol/L concentrations of RU486 and 10^{-6} mol/L dexamethasone, the final cell number decreased by 53% compared to that of cells treated only with dexamethasone at 10^{-6} mol/L.

TABLE 2. Influence of treatment *in vivo* with RU486 (0.5 mg/day) for 4 weeks on the concentrations of receptors for estradiol, progesterone, glucocorticoids, and EGF in U87MG human brain tumors xenografted in nude mice

	Type of receptor protein[a]			
	Estradiol	Progesterone	Glucocorticoid	EGF
Control	7.3 ± 1.8	3.0 ± 0.6	159.7 ± 19.2	113.7 ± 14.4
RU486	12.3 ± 3.4	3.0 ± 1.3	34.1 ± 5.7[b]	154.7 ± 61.2

[a] Concentration expressed as femtomoles per mg cytosol protein for the steroid hormones and as femtomoles per mg membrane protein for EGF receptors. Significance was calculated with Duncan's new multiple range test. Values represent the mean ± SEM.
[b] $P < 0.01$ *vs.* controls.

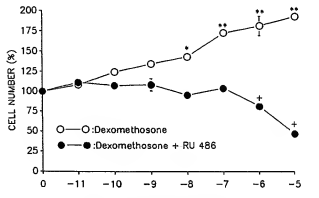

FIG. 4. Influence of dexamethasone and RU486 administreton on proliferation of U87MG human malignant glioma cells. Dexamethasone concentrations ranged from 10^{-11}–10^{-6} mol/L (○); RU486 concentrations ranged from 10^{-11}–10^{-6} mol/L in the presence of dexamethasone at a concentration of 10^{-6} mol/L (●). Statistical significance was calculated by Duncan's new multiple range test. *Vertical bars* represent the SEM. *, $P < 0.05$; **, $P < 0.01$ (*vs.* control). +, $P < 0.01$ (*vs.* 10^{-6} mol/L dexamethasone group).

The stimulatory effect of dexamethasone on tumor growth observed in our study is in agreement with the findings of other reports, which indicated that glucocorticoid hormones can augment the growth of malignant glioma cells in cell culture (4, 9, 10). Tumors obtained from patients who had received pharmacological doses of dexamethasone before

craniotomy were reported to grow considerably faster *in vitro* than tumors from patients who had not been given this drug (26).

It appears that glucocorticoid-like compounds stimulate brain tumor growth only in the presence of GR (4). Our findings showing that the stimulatory effect of dexamethasone on malignant glioma cell proliferation could be suppressed by RU486 support the view that the mechanism by which glucocorticoid hormones modify cell growth is mediated through specific GR. It has been previously demonstrated that RU486 abolished the effects of dexamethasone in L-929 mouse fibroblasts *in vitro* (27).

Glucocorticoid hormone administered in supraphysiological doses has been reported to exert antiproliferative effects on different neuroepithelial tumors cultured *in vitro* (9, 10) and on human glial tumors treated *in vivo* (19, 28). However, treatment of patients with malignant gliomas with high doses of methylprednisolone in a randomized trial failed to improve survival time (29). The mechanism of the inhibitory effect of supraphysiological doses of glucocorticoid hormones on cell growth remains unclear, although several hypotheses can be put forward. This inhibition could be brought about by down-regulation of GR [human GR cDNA contains sequences sufficient for receptor down-regulation (21)], by membrane alteration, as demonstrated for tamoxifen in human breast cancer cells (30), or by induction of a more differentiated state of cells and enhancement of the normal cell-cell interaction (31).

Our study suggests that the steroid hormone antagonist RU486 may be of potential clinical value in the treatment of malignant gliomas. Long term clinical therapy with RU486 in patients with unrespectable meningiomas (>1 yr) indicated that life-threatening adrenal insufficiency does not develop (13, 14). However, the suppression by RU486 of the negative feedback activity of corticoids provokes an increase in ACTH, which activates steroidogenesis (15). The resulting increase in levels of cortisol may require treatment with higher doses of RU486 to overcome this effect (15). The elevation of sex steroid hormones that is also produced is probably not detrimental to patients with malignant gliomas, as sex hormone receptor levels are usually low in this kind of tumor (5, 20).

In conclusion, our results suggest that the steroid hormone antagonist RU486 has significant potential as a therapeutic agent in the treatment of malignant gliomas, but the exact clinical regimens need to be established.

Acknowledgments

We thank Ivan Lopez for his technical assistance, Roussel-UCLAF (Romainville, France) for RU486, and Prof. E. E. Baulieu for valuable advice.

References

1. **Boring** CC, **Squires** TC, **Tong** T. 1992 Cancer statistics. Ca-A Cancer J Clin. 42:19–38.
2. **Davis DL, Hoel D, Percy C, Ahlbom A, Schwartz J.** 1990 Is brain cancer mortality increasing in industrial countries? Ann NY Sci 609:191–204.
3. **Ellemann K, Christensen L, Gjerris F, Briand P, Kruse-Larsen C.** 1988 Glucocorticoid receptors in glioglastoma multiforme: a new approach to antineoplastic glucocorticoid therapy. Acta Neurochir. 93:6–9.
4. **Paoletti P, Butti G, Zibera C, et al.** 1990 Characteristics and biological role of steroid hormone receptors in neuroepithelial tumors. J Neurosurg. 73:736–742.
5. **Stojkovic RR, Jovancevic M, Santel DJ, Grcevic N, Gamulin S.** 1990 Sex steroid receptors in intracranial tumors. Cancer. 65:1968–1970.
6. **Cahill DW, Basirelahi N, Solomon LW, Dalton T, Saloman M, Ducker TB.** 1984 Estrogen and progesterone receptors in meningiomas. J Neurosurg. 60:985–993.
7. **Concolino G, Giuffre R, Margiotta G, Liccardo G, Marocci A.** 1984 Steroid receptors in CNS: estradiol (ER) and progesterone (PR) receptors in human spinal cord tumors. J Steroid Biochem. 20:491–494.
8. **Knerich R, Scerrati M, Butti G.** 1987 Steroid hormone receptors and intracranial tumors. In: Chatel M, Darcel F, eds. Brain oncology. Dordrecht: Martinus Nijhoff; 159–163.
9. **Freshney RI, Sherry A., Hassanzadah M, Freshney M, Crilly P, Morgan D.** 1980 Control of cell proliferation in human glioma by glucocorticoids. Br J Cancer. 41:857.
10. **Mealy J Jr, Chen TT, Schanz GP.** 1971 Effects of dexamethasone and methylprodnisolone on cell cultures of human glioblastomas. J Neurosurg. 34:324–334.
11. **Poisson M,.** 1984 Steroid receptors in human meningiomas. Clin Neuropharmacol. 7:320–324.
12. **Brentani MM, Lopes MTP, Martins VR, Plese JPP.** 1984 Steroid receptors in intracranial tumors. Clin Neuropharmacol. 7:347–350.
13. **Lamberts SWJ, Koper JW, de Jong FH.** 1991 The endocrine effects of long-term treatment with mifepristone (RU 486). J Clin Endocrinol Metab. 73:187–191.
14. **Grunberg SM, Weiss MH, Spitz IM, et al.** 1991 Treatment of unresectable meningiomas with the antiprogesterone agent mifepristone. J Neurosurg. 74:861–866.
15. **Baulieu EE.** 1991 The steroid hormone antagonist RU486. Mechanism at the cellular level and clinical applications. Endocrinol Metab Clin North Am. 20:873–891.
16. **Steel RGD, Torrie J.** 1960 Principles and procedures of statistics. New York: McGraw-Hill; 114.
17. **Sekalovic G, Wittliff JL, Schally AV.** 1990 Detection and partial characterization of receptors for [D-Trp^6]-luteinizing hormone-releasing hormone and epidermal growth factor in human endometrial carcinoma. Cancer Res. 50:1841–1846.
18. **Halmos G, Schneider G, Falkay G.** 1991 Advances in steroid analysis '90. In: S. Gorog (D.S. Gorog), ed. Budapest: Academic Publishing House Bp.; 37–42.
19. **Pasic R, Djulbegovic B, Wittliff JL.** 1990 Comparison of sex steroid receptor determinations in human breast cancer by enzyme immunoassay and radioligand binding. J Clin Lab Anal. 4:430–436.
20. **Kornblum JA, Bay JW, Gupta MK.** 1988 Steroid receptors in human brain and spinal cord tumors. Neurosurgery. 23:185–188.
21. **Ellemann K, Gollinger B, Soerensen PS, Zeeberg I.** 1988 The antineoplastic effect of methylprodnisolone pulse therapy in two patients with glucocorticoid receptor-positive glioblastoma multiforme. Acta Neurol Scand. 77:74–77.
22. **Baulieu EE.** 1991 The antisteroid RU486. Its cellular and molecular mode of action. Trends Endocrinol Metab. 2:233–239.
23. **Bamstein KL, Jewell CM, Cidlowski JA.** 1990 Human glucocorticoid receptor cDNA contains sequences sufficient for receptor down-regulation. J Biol Chem. 265:7284–7291.
24. **Modiano JF, Kokai Y, Weiner DB, Pykett MJ, Nowell PC, Lyttle CR.** 1991 Progesterone augments proliferation induced by epidermal growth factor in a feline mammary adenocarcinoma cell line. J Cell Biochem. 45:196–206.
25. **Schally AV.** 1988 Oncological applications of somatostatin analogs. Cancer Res. 48:6977–6985.
26. **Sherbet GV, Lakshimi MS, Hoddad SK, Chir B.** 1977 Does dexamethasone inhibit the growth of human gliomas? J Neurosurg. 47:864–870.
27. **Jung-Testas I, Baulieu EE.** 1983 Inhibition of glucocorticosteroid action in cultured L-929 mouse fibroblasts by RU486, a new anti-

glucocorticosteroid of high affinity for the glucocorticosteroid receptor. Exp Cell Res. 147:177–182.
28. **Leiguarda R, Sierra J, Pardal C, Zambrano D.** 1985 Effect of large doses of methyprednisolone on supratentorial intracranial tumors. Eur Neurol. 24:23–32.
29. **Green SB, Byar SP, Walker MD, et al.** 1983 Comparison of carmustine, procarbazine, and high-dose methylprednisolone as additions to surgery and radiotherapy for the treatment of malignant glioma. Cancer Treat Rep. 67:121–132.
30. **Sica G, Natoli V, Marchetti P, Piperno S, Iacobelli S.** 1984 Tamoxifen-induced membrane alteration in human breast cancer cells. J Steroid Biochem. 20:425–428.
31. **Freshney RI.** 1984 Effects of glucocorticoids on glioma cells in culture. Minireview on cancer research. Exp Cell Biol. 52:286–292.

Exhibit 5

Induction of Thymidine Phosphorylase in Both Irradiated and Shielded, Contralateral Human U87MG Glioma Xenografts: Implications for a Dual Modality Treatment Using Capecitabine and Irradiation[1]

Carmelo Blanquicett, G. Yancey Gillespie, L. Burt Nabors, C. Ryan Miller, Sumen Bharara, Donald J. Buchsbaum, Robert. B. Diasio, and Martin R. Johnson[2]

Departments of Pharmacology and Toxicology, Division of Clinical Pharmacology [C. B., R. B. D., M. R. J.]; Surgery, Division of Neurosurgery [G. Y. G., S. B., C. R. M.], Neurology [L. B. N.], and Radiation Oncology, Division of Radiation Biology [C. R. M., D. J. B.]; and Comprehensive Cancer Center [C. B., D. J. B., R. B. D., M. R. J.], University of Alabama at Birmingham, Birmingham, Alabama 35294

Abstract

In the United States, tumors of the central nervous system remain the third leading cancer-related cause of death in young adults with a median survival time of <1 year. A recent case study suggested that Capecitabine (a novel, fluoropyrimidine prodrug) may be effective in the treatment of brain metastases. Pharmacogenomic studies have correlated the antitumor response to Capecitabine with the expression of the drug metabolizing enzymes thymidine phosphorylase (TP) and dihydropyrimidine dehydrogenase (DPD). In the current study, we examined TP and DPD expression in normal human brain tissues and in glioblastoma multiforme, the most common and malignant type of brain tumor. Because previous reports suggest a tumor necrosis factor (TNF)-α-mediated increase in TP expression after irradiation (a current standard of care for glioblastoma multiforme), we also examined the effect of irradiation on the expression of TP, DPD, and TNF-α in both irradiated and lead-shielded contralateral U87MG glioma xenografts within the same animal. Expression levels were determined using real-time quantitative PCR as described previously. Results demonstrate an ~70-fold increase in TP mRNA levels 4 days after irradiation, relative to initial control levels. Interestingly, TP mRNA in the lead-shielded tumors (contralateral to irradiated tumors) increased ~60-fold by day 10 relative to initial control levels. Elevated TP levels were sustained for 20 days in irradiated xenografts but began to decrease after 15 days in the shielded/contralateral tumors, returning to baseline by 20 days. TP mRNA levels in normal mouse liver were unaltered, suggesting a tumor-associated effect. TNF-α mRNA levels did not increase after irradiation; therefore, mRNA expression of 11 additional cytokines [interleukin (IL)-1α, IL-1β, IL-2, IL-4, IL-5, IL-8, IL-10, IL-12p35, IL-12p40, IL-15, and IFN-γ] in both the irradiated and shielded xenografts was quantitated. Results demonstrated increased levels of IFN-γ, IL-10, and IL-1α by 6.3-, 3.7-, and 1.6-fold, respectively, in irradiated tumors only. DPD mRNA levels did not change after irradiation. The tumor-associated induction of TP in irradiated and lead-shielded tumors within the same animal may have significant implications for the combined modality treatment of cancer patients with Capecitabine in conjunction with radiotherapy and may apply to the treatment of distant tumors and or metastatic disease.

Introduction

In the United States, tumors of the central nervous system remain the most prevalent solid neoplasm of childhood and the third leading cancer-related cause of death in adolescents and adults between the ages of 15 and 34 years (1). Unfortunately, despite over 50 years of research (including highly aggressive therapeutic approaches), the median survival of patients with malignant brain tumors remains <1 year (2, 3). GBM[3] remains the most common and malignant type of brain tumor and is characterized by an unusual resistance to treatment with both radiation and chemotherapy. Nitrosourea agents such as 1,3-bis(2-chloroethyl)-1-nitrosourea are frequently used concurrently with radiotherapy (4, 5); unfortunately, severe dose-related toxicity limits the usefulness of these compounds (6). Although chemotherapy agents have not generally demonstrated survival benefit in this disease, a recently published case report suggested that Capecitabine might be an effective treatment for brain metastases (7).

Capecitabine is a recently introduced oral prodrug that is converted into 5-FU by three sequential enzymatic steps. TP is the final and rate-limiting enzyme responsible for Capecitabine activation (8–10). Once converted into 5-FU, metabolism results in either: (*a*) anabolism into cytotoxic nucleotides, which are ultimately responsible for tumor cell death; or (*b*) catabolism into biologically inactive metabolites that are ex-

Received 6/6/02; revised 8/19/02; accepted 8/27/02.
[1] Supported by NIH Grant CA85381.
[2] To whom requests for reprints should be addressed, at Department of Clinical Pharmacology, 1824 6th Avenue South, Wallace Tumor Institute, Room 620, University of Alabama at Birmingham, Birmingham, AL 35294-3300. Phone: (205) 975-8435; Fax: (205) 975-5650; E-mail: Martin.Johnson@ccc.uab.edu.

[3] The abbreviations used are: GBM, glioblastoma multiforme; 5-FU, 5-fluorouracil; IL, interleukin; TNF, tumor necrosis factor; TP, thymidine phosphorylase; DPD, dihydropyrimidine dehydrogenase.

Table 1 Primer and probe sequences and optimal concentrations

Target	Sequence	Optimal conc. (nM)
TP (human)		
Fwd	GGAGAAGGGTGACCGACTCA	100
Probe	FAM-CGCTGAGATCAATCGGCCCGACTAT-TAMRA	200
Rev	TGCCCAGACTCGGCAAAG	200
TP (mouse)		
Fwd	CGGCCAGAGTGCAAAGCT	200
Probe	FAM-CAGCATACAGGATCCCATCAGCAGGAA-TAMRA	200
Rev	TCCACAGTGGCTGTCACATCTC	300
TNF-α		
Fwd	GGAGAAGGGTGACCGACTCA	300
Probe	FAM-CGCTGAGATCAATCGGCCCGACTAT-TAMRA	250
Rev	TGCCCAGACTCGGCAAAG	200
S9		
Fwd	ATCCGCCAGCGCCATA	100
Probe	FAM-AGCAGGTGGTGGTGAACATCCCGTCCTT-TAMRA	300
Rev	TCAATGTGCTTCTGGGAATCC	100
DPD		
Fwd	CCAAAGGCAGTAAAGCAGGAA	300
Probe	FAM-TGCGCCTGTCACTCTCCATTGCC-TAMRA	25
Rev	TCACGACTCCCCGTATCGA	100

creted in the urine and bile (11). Pharmacokinetic studies have shown that the amount of 5-FU available for anabolism is determined by the extent of its catabolism (11, 12). Thus, a delicate balance exists between the enzymatic activation of Capecitabine into 5-FU (catalyzed by TP) and its catabolic elimination (catalyzed by DPD). Several studies evaluating Capecitabine have demonstrated that intratumoral levels of TP and DPD (expressed as a TP/DPD ratio) are the best indicators of tumor response with increased efficacy characterized by high TP expression (increased conversion of Capecitabine into 5-FU) and low DPD expression (decreased inactivation of 5-FU; Refs. 13–15). In addition, a recent clinical study suggests that high TP expression is a good indicator of disease-free survival for those patients taking 5-FU prodrug-based chemotherapy, with patients expressing high TP and low DPD demonstrating the best disease-free survival (16)

Induction of TP has been suggested as a potential method of increasing efficacy of Capecitabine. Several cytokines (IL1-α, TNF-α, IFN-γ) and anticancer drugs (paclitaxel, docetaxel, cyclophosphamide) have been shown to increase TP expression (17–19). Of particular importance, irradiation has been shown to result in increased TP expression with a concurrent increase in Capecitabine efficacy (20). Because irradiation remains a current standard of care for the treatment of GBM, the addition of Capecitabine represents a rational and potentially synergistic combination.

In this study, we quantitated TP and DPD mRNA expression levels in GBM and normal human brain tissue. The effect of irradiation on the expression of TP, DPD, and several cytokines in contralateral irradiated and lead-shielded U87MG glioma xenograft tumors was also examined. The combined modality treatment of Capecitabine and irradiation may have significant implications for tumor response, which could extend to distant or metastatic tumors and, ultimately, result in prolonged patient survival.

Materials and Methods

Tissue Preparation. After an Institutional Review Board-approved protocol (X980409003), GBM and normal brain tissue samples were obtained from cancer patients undergoing surgical resection. Tissues used for RNA extraction had been snap frozen and stored at −70°C. A representative sample of the tissue obtained was fixed, paraffin-embedded, sectioned, and stained with H&E so that it could be examined by a neuropathologist to establish a diagnosis.

RNA Extraction. Total RNA was isolated as described previously (21, 22). All sample concentrations were calculated spectrophotometrically at A^{260} and diluted to a final concentration of 20 ng/μl in RNase-free water containing 12.5 ng/μl of total yeast RNA (Ambion, Austin, TX) as a carrier.

Real-Time Quantitative PCR. Expression levels were determined using an ABI 7700 Sequence Detection System as previously described by our laboratory (21, 22). Before sample analyses, housekeeping gene variation was determined for GBM and normal brain tissue as previously described by our laboratory (21). The primers and probes for human TP, DPD, TNF-α, S9 ribosomal RNA (GenBank accession no. NM001953, U20938, M10988 and NM001013 respectively) and mouse TP (GenBank accession no. AW744006) were designed using the Primer Express software (Applied Biosystems, Foster City, CA). The sequence and optimum primer/probe concentrations are shown in Table 1. Expression levels were calculated using the relative standard curve method as described previously (21, 22). All reactions were run in triplicate, and standard curves with correlation coefficients falling <0.98 were repeated. Control reactions confirmed that no amplification occurred when yeast total RNA was used as a template or when no-template control reactions were performed.

Cell Culture. U87MG glioma cells (purchased from the American Type Culture Collection, Manassas, VA) were

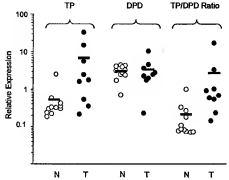

Fig. 1. Expression of TP and DPD in GBM (T) and normal brain (N) tissue. As shown above, TP expression is higher in GBM ($n = 9$) as compared with normal brain ($n = 11$) with a mean difference of 6.2 (SD = 7.2; $P = 0.13$). There was no significant difference in DPD expression levels in the same tissue samples (mean difference of 0.32; SD = 2.13; $P = 0.76$). The average TP/DPD ratio demonstrated in GBM (2.69) is ~16-fold higher than that of normal brain tissue (0.17) and is primarily because of TP overexpression in GBM. This profile should result in selective conversion of Capecitabine in tumor compared with normal brain tissues (16-fold higher TP/DPD ratio in GBM relative to normal brain).

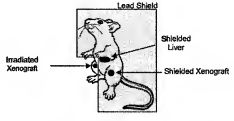

Fig. 2. Schematic of mouse xenograft location(s) and irradiation. One of the two flanks containing a U87MG glioma xenograft was irradiated, whereas the contralateral flank (containing the other U87MG xenograft) as well as the body of the mouse (including the mouse liver) was lead shielded.

maintained in stationary monolayer cultures at 37°C and 5% CO_2 in a humidified atmosphere using a 50:50 mixture of DMEM and Ham's Nutrient Mixture F12 supplemented with 7% heat-inactivated fetal bovine serum and 2.6 mM L-glutamine. All cell cultures were maintained in antibiotic-free conditions and regularly checked for *Mycoplasma* contamination using a PCR-based kit (ATCC). Near confluent (75%) monolayers of cells were harvested by brief exposure to 0.05% trypsin/0.53 mM EDTA (Life Technologies, Inc. Gaithersburg, MD). Harvested cells were pelleted (200 × *g*, 8 min at ambient temperature) in complete medium and resuspended in serum-free medium. Viable cells were counted using a Neubauer hemacytometer using trypan blue (0.4%) exclusion. To determine whether IFN-γ induced TP transcription, 0.5 ng/μl IFN-γ were added to 1×10^6 U87MG glioma cells and omitted in the control population. Cells were incubated for 24 h and collected as described above for RNA isolation.

Human Cancer Xenograft Preparation and Irradiation. Athymic, nude NCr mice (nu/nu) were anesthetized with ketamine/xylozine and s.c. injected bilaterally into hind flanks with a suspension of 5×10^6 U87MG glioma cells. Tumors were allowed to develop between 200 and 400 mm^3 in size. Mice were randomized into control and treatment groups, and one of the glioma tumor-bearing flanks of the treated group was irradiated, whereas the rest of the body (including the tumor in the opposite flank) was lead shielded (Fig. 2). Irradiation was carried out using a ^{60}Co teletherapy X-ray unit (Picker, Cleveland, OH) at a dose of 8.5 Gy. Mice in control groups were anesthetized before the irradiation but were not irradiated. Mice were sacrificed between 0–20 days after irradiation.

Cytokine Expression. The effect of irradiation on the expression of 12 cytokines (IL-1α, IL-1β, IL-2, IL-4, IL-5, IL-8, IL-10, IL-12p35, IL-12p40, IL-15, IFN-γ, and TNF-α) in the U8MG glioma xenografts was examined using a Taqman Cytokine Gene Expression Plate I (Applied Biosystems) according to manufacturer's instruction. Nonirradiated U87MG glioma xenografts in control mice were used as the calibrator.

Statistical Analyses. Statistical analyses were performed using Student's *t* test where differences were considered to be significant when $P < 0.05$.

Results

Quantitation of TP and DPD Expression in GBM and Normal Brain Tissues. Before quantitation using real-time quantitative PCR, we examined the variability of 12 housekeeping genes in GBM and normal brain tissues as previously described by our laboratory (21). The housekeeping genes examined include: *18S ribosomal RNA*; *β-glucuronidase*; *β2-microglobulin*; *β-actin*; *S9 ribosomal RNA*; *acidic ribosomal protein*; *TATA binding protein*; *transferrin receptor*; *glyceraldehyde 3-phosphate dehydrogenase*; *cyclophilin*; *phosphoglycerokinase*; and *hypoxanthine ribosyl transferase*. On the basis of these analyses, the ribosomal S9 gene (which demonstrated <1.5-fold variation in expression between normal and tumor tissues) was used to normalize the amount of total RNA in each sample (data not shown).

As shown in Fig. 1, TP expression is higher in GBM (T) as compared with normal brain tissue (N) with a mean difference of 6.2 (SD = 7.2; $P = 0.13$). Furthermore, this data suggests more variability of TP expression among tumor samples (ranging from a low of 0.21 to a high of 33.01) as compared with normal brain tissue (ranging from a low of 0.18 to a high of 2.47). There was no significant difference in DPD levels between normal and tumor tissue samples (mean difference of 0.32; SD = 2.13; $P = 0.76$). The average TP/DPD ratio demonstrated in GBM (2.69) is ~16-fold higher than that of normal brain tissue (0.17). The higher TP/DPD ratio in GBM is primarily because of higher expression of TP in GBM (6.72) compared with normal brain tissue (0.52) because there was no significant difference in DPD levels in the same tissues (3.33 and 3.01, respectively).

TP, DPD, and TNF-α Expression in U87MG Xenografts. As described in the "Materials and Methods" and illustrated in Fig. 2, athymic NCr nude mice were given injections of glioma cells in both hind flanks and allowed to develop tumors. One of the tumor-bearing flanks of the treated group was irradiated, whereas the rest of the mouse was lead shielded (Fig. 2). As shown in Fig. 3*A*, TP mRNA levels did not

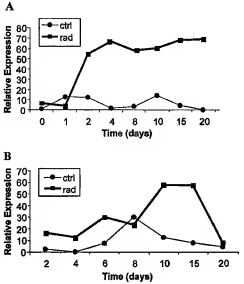

Fig. 3. TP expression in irradiated and shielded U87MG glioma xenografts in mice. *A*, as shown above, TP mRNA levels increased ~70-fold in irradiated tumors relative to nonirradiated tumors in control mice, remaining elevated 20 days after irradiation. *B*, of particular interest, TP mRNA levels in the shielded tumors (in the same animal) increased ~60-fold (relative to initial control levels) 10 and 15 days after irradiation before dropping to control levels at 20 days. *Error bars* have been incorporated into this figure but are so small as to be obscured by the data point.

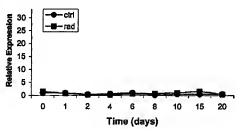

Fig. 4. TP expression in shielded normal mouse liver. Mouse TP mRNA expression in normal liver was evaluated in shielded and nonirradiated (control) mice. As shown above, there is no significant difference between shielded and nonirradiated mouse liver TP mRNA levels. *Error bars* have been incorporated into this figure but are so small as to be obscured by the data point.

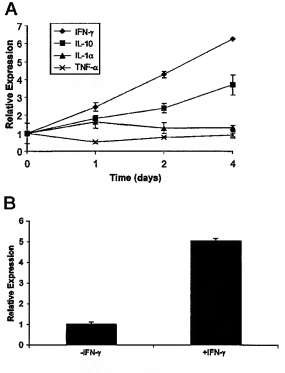

Fig. 5. *A*, effect of irradiation on mRNA expression of 12 cytokines. Cytokine expression in irradiated tumors (days 0–4 after irradiation) was determined for 12 cytokines using a TaqMan Cytokine Gene Expression Plate I as described in "Materials and Methods." As shown above, IFN-γ demonstrated the greatest increase in expression (6.3-fold) followed by IL-10 (3.7-fold) in irradiated xenografts relative to control xenografts at 4 days after irradiation. IL-1α demonstrated a <2-fold increase in expression 24 h after irradiation (1.6-fold), returning to baseline levels 2–4 days after irradiation. TNF-α levels (included in the cytokine plate) did not increase above baseline. IL-2, IL-4, IL-5, and IL-8, which are not shown, did not demonstrate any increases in expression after irradiation. IL-1β, IL-12p35, IL-12p40, and IL-15 mRNA levels were beyond the limits of detection in all of the samples (data not shown). *B*, quantitation of TP in U87MG glioma cells without (–) and with (+) IFN-γ. TP expression (mRNA levels) increased 5-fold in the U87MG glioma cells treated with IFN-γ (+) as compared with untreated cells (–), suggesting a direct effect of IFN-γ on TP transcription.

increase during the first 24 h after irradiation. However, by day 2, TP mRNA levels in irradiated tumors rapidly increased, peaking at day 4 with a ~70-fold increase relative to initial, nonirradiated tumors in control mice. As shown in Fig. 3*A*, the increase in TP mRNA levels was maintained in irradiated tumors for up to 20 days after irradiation (mean difference of 39.31; SD = 18.5; $P < 0.001$) and was an average 10-fold higher than control (nonirradiated) tumors.

TP mRNA in the lead-shielded tumor (from the contralateral flank of the same mouse) did not increase during the first 8 days after irradiation (Fig. 3*B*). However, by days 10 and 15, TP mRNA levels increased ~60-fold relative to initial TP mRNA levels in nonirradiated tumors in control mice (mean difference of 18.07; SD = 16.2; $P = 0.04$). Unlike the irradiated tumors, TP mRNA levels in the shielded tumors decreased to control levels 20 days after irradiation (Fig. 3*B*). No significant change in either DPD (mean difference of 0.13; SD = 0.56; $P = 0.61$) or TNF-α (mean difference of 0.45; SD = 1.2; $P = 0.41$) expression was observed in either the irradiated or shielded tumors relative to control tumors (data not shown).

TP Expression in Shielded Mouse Liver. To determine whether the increase in TP mRNA levels in the shielded xenografts was tumor associated, we examined mouse TP expression in liver tissue from treated (irradiated) and control (nonirradiated) mice. These analyses demonstrated no significant differences in mouse liver TP mRNA levels (mean difference of 0.21; SD = 0.39; $P = 0.24$) between irradiated mice and control mice (Fig. 4) over the time course studied, suggesting that the increase in TP mRNA seen in the xenografts was tumor associated.

Cytokine Expression in U87MG Xenografts. The delay between irradiation and the increase in TP mRNA levels (4 and 10 days in irradiated and shielded xenografts, respectively) suggests a secondary-mediated induction of TP rather than a direct effect. Because several cytokines, which have been shown to increase after irradiation, have also been shown to increase TP, we evaluated the expression of 12 cytokines (including IL-1α, IL-1β, IL-2, IL-4, IL-5, IL-8, IL-10, IL-12p35, IL-12p40, IL-15, IFN-γ, and TNF-α) at several days preceding elevated levels of TP mRNA (days 0, 1, 2, and 4 in irradiated tumors and days 0, 4, 6, and 10 in shielded tumors). As shown in Fig. 5*A*, irradiated xenografts demonstrated the greatest increase in expression of IFN-γ (6.3-fold) followed by IL-10 (3.7-fold) at 4 days after irradiation and relative to nonirradiated xenografts. IL-1α demonstrated a <2-fold increase in expression 24 h after irradiation (1.6-fold), returning to baseline levels 2–4 days after irradiation. TNF-α levels (included in the commercially available cytokine plate) did not increase above baseline levels, agreeing with results from our independently designed primers and probes (see above). Expression levels of IL-2, IL-4, IL-5, and IL-8 did not increase after irradiation but were detectable, whereas IL-1β, IL-12p35, IL-12p40, and IL-15 mRNA levels were undetectable in both irradiated and control xenografts.

Cytokine expression was also examined in contralateral, shielded tumors (see Fig. 2) and compared with tumors in nonirradiated mice on days 0, 4, 6, and 10. Of the 12 cytokines examined, TNF-α and IL-10 demonstrated <2-fold increases in expression on days 4 and 6. Although IL-8 and IL-1α mRNA levels were detected in the shielded tumors, no increases were observed with these cytokines (data not shown). The remaining cytokines were below the limits of detection (IL-1β, IL-2, IL-4, IL-5, IL-12p35, IL-12p40, IL-15, and IFN-γ).

Induction of TP Expression in Cultured U87MG Cells with IFN-γ. To determine whether IFN-γ alone can induce TP transcription, U87MG glioma cells were incubated with IFN-γ for 24 h. As shown in Fig. 5*B*, TP mRNA increased 5-fold compared with control cells.

Discussion

Despite highly aggressive therapeutic approaches, the median survival of 1 year for patients with malignant brain tumors has not appreciably changed in the last 50 years (1–3). Recent advances in the molecular analysis of tumor tissue that allow quantitation of drug-metabolizing enzymes have resulted in the ability to predict response to chemotherapy (22–27). Although previous studies have suggested that this pharmacogenomic approach can be used to increase efficacy through selection of a subpopulation of patients likely to respond to chemotherapy (13–15, 27), a broader approach would be to design novel therapies based on the molecular profile of the tumor type.

A recent study reported the effective use of Capecitabine for brain metastases originating from breast cancer (7). The partial response (shown by decreased lesion size and improved mental performance) was particularly noteworthy because previous hormonal treatment, whole brain irradiation, and systemic chemotherapy, including treatment with 5-FU, proved ineffective. In addition to providing a potentially effective treatment for brain metastases, this study demonstrated that: (*a*) tumor resistance to 5-FU does not preclude effective treatment with Capecitabine; and (*b*) Capecitabine can reach therapeutic concentrations in brain tumor tissues. Because response to Capecitabine has been correlated to intratumoral expression of TP and DPD (expressed as a TP:DPD ratio; Refs. 13–15, 27), we examined the expression of these drug-metabolizing enzymes in GBM and normal human brain tissues. In addition, the effects of irradiation on TP mRNA expression were examined in both irradiated and shielded, contralateral U87MG glioma xenografts.

As shown in Fig. 1, the average TP/DPD ratio in GBM is ~16-fold higher than in normal brain tissue. This increased TP/DPD ratio is primarily because of higher TP expression in tumor compared with normal brain tissue. There was no significant difference in DPD expression levels between normal and tumor tissues. This distribution of TP and DPD should result in selective intratumor activation of Capecitabine (*i.e.*, intratumoral 5-FU levels would be higher than normal tissue), whereas 5-FU clearance from tumor and normal tissues should be similar (equivalent DPD expression). Furthermore, these data suggest that in GBM and normal brain tissue samples, TP and DPD appear to be independent determinants of response with no apparent correlation in expression levels. Interestingly, the variability of TP expression is much higher in GBM as compared with normal brain tissue. However, whether this variability correlates to other factors such as tumor stage, location, or patient survival remains to be determined.

Recent studies have shown that it is possible to increase Capecitabine efficacy by induction of TP (20). Although irradiation has been shown to result in increased TP levels with a concurrent increase in Capecitabine efficacy in colon, cervix, gastric, and breast cancer xenograft models (20), the effects of irradiation in glioma xenograft models have not been examined before this study. As shown in Fig. 3*A*, irradiation increased TP mRNA expression ~70-fold relative to initial control (nonirradiated) levels. Shielded contralateral tumors demonstrated a 60-fold increase in TP expression between 10 and 15 days after irradiation (Fig. 3*B*). Because DPD levels were unaffected, this results in a 70- and 60-fold increase in the TP/DPD ratio for these tumors, respectively.

The current trend in treatment is to reduce the amount of neurotoxicity from whole brain radiation by focusing the irradiation to the area of residual tumor or the site of tumor excision (involved fields or intensity-modulated radiation therapy). However, recurrence is common, generally within a few centimeters of the original tumor site (just beyond the irradiated field; Ref. 28). The contralateral xenograft model used in this study (Fig. 2) was designed to represent invasive, metastatic, and/or micrometastatic tumors in humans. The induction of TP in shielded tumors that were not directly irradiated has potential implications for improving Capecitabine efficacy in patients with invasive tumors that were not directly irradiated during treatment. Furthermore, examination of shielded mouse liver TP (Fig. 4) agrees with previous studies, suggesting that the induction of TP is a tumor-

associated effect (20). Interestingly, TNF-α mRNA levels did not increase after irradiation (Fig. 5).

The molecular basis for induction of TP after irradiation remains to be elucidated. Although a previous study suggests that increased TNF-α levels after irradiation results in increased TP expression, no increase in TNF-α was observed in these glioma xenografts. Examination of Fig. 3 reveals that elevated TP mRNA levels occurred at 4 and 10 days in irradiated and shielded tumors, respectively. This delayed increase in TP mRNA levels suggests a mediated and potentially complex mechanism with induction possibly involving a currently unidentified, soluble cell factor(s). The sustained increase in TP mRNA levels (particularly in irradiated tumors by up to 20 days) may also be suggestive of other mechanisms involved such as stabilization of the TP mRNA transcript. Because IL-1α and IFN-γ have also been shown to induce TP (17–19), we examined the expression of 12 cytokines (IL-1α, IL-1β, IL-2, IL-4, IL-5, IL-8, IL-10, IL-12p35, IL-12p40, IL-15, IFN-γ, and TNF-α) in irradiated and shielded glioma xenografts (Fig. 5A). Although significant changes were not detected in most of the cytokines examined, IFN-γ, IL-10, and IL-1α mRNA levels increased 6.3-, 3.7-, and 1.6-fold, respectively. In fact, IFN-γ has been shown to induce the highest levels of TP expression relative to TNF-α and IL-1α in human macrophages with gamma-activated sequence elements in the TP promoter being essential for IFN-γ-dependent activation of the TP gene (29). In the current study, we demonstrate that IFN-γ induced TP mRNA levels in U87MG glioma cells (Fig. 5B). Taken collectively, these studies suggest that the molecular basis for the induction of TP after irradiation may vary depending on tumor type with at least two mechanisms: (a) a TNF-α-independent mechanism (as demonstrated in the glioma xenograft models); or (b) a TNF-α-dependent mechanism [as demonstrated in the in colon, cervix, gastric, and breast cancer xenograft models (20)]. In addition, increased IFN-γ levels have been shown to have antitumor activity in recurrent gliomas by inhibition of angiogenesis, apoptosis of endothelial cells, suppression of glioma growth, and decreased cell proliferation (30, 31). These studies suggest the potential use of IFN-γ to induce TP expression in patients treated with Capecitabine (where irradiation is not a treatment option) or as an addition to the combination of Capecitabine and irradiation.

Previous studies have shown induction of IL-10 (a potent anti-inflammatory cytokine) after irradiation (32). In addition, immunohistochemical staining has suggested that elevated IL-10 protein levels correlate with elevated TP expression in a study examining oropharyngeal carcinoma (33). The data presented in this study suggest that increased IL-10 expression precedes increased TP levels. Interestingly, IL-10 has been reported to suppress TNF-α (34). Additional studies will need to examine whether the increased levels of IL-10 observed in this study are related to the lack of increase in TNF-α mRNA levels in irradiated xenografts. The increase in IL-1α after irradiation that was observed in this study is in agreement with studies that have also implicated IL-1α in TP up-regulation (20). However, only a slight increase in IL-1α (<2-fold) during the first 24 h after irradiation was observed. Future *in vitro* studies will examine the role of these cytokines in the molecular basis for TP induction after irradiation.

Although, chemotherapy has not yet emerged as a standard of care for brain tumors, a recent case study reports the successful treatment of brain metastasis with Capecitabine (7). Because ~24% of human cancers are known to metastasize to the brain (35), this may provide a new and potentially effective treatment option in a disease where incidence is increasing and median survival remains poor. However, whether this same approach can be used for primary brain tumors such as GBM remains to be determined. Molecular analysis of patient samples suggest that the high TP:DPD ratio (the determinant of response to Capecitabine) in GBM compared with normal brain tissue would result in the preferential intratumor activation of Capecitabine. In addition, irradiation (a standard of care for the treatment of GBM) is shown to produce a tumor-associated induction of TP expression, which could result in improved Capecitabine efficacy. Most importantly, the induction of TP is shown to occur in distant (nonirradiated) tumors in the same animal. Although the combination of 5-FU plus radiotherapy has been shown to produce additive efficacy, preclinical studies in xenograft models suggest that the effect of Capecitabine plus radiotherapy is synergistic (18, 20, 36). In addition, because 5-FU is a well-established radiosensitizing agent, potentially higher intratumoral levels of 5-FU (achieved by higher intratumoral TP levels) represent an opportunity to maximize the antitumor efficacy through the careful optimization of timing, dose, and administration of Capecitabine and irradiation. The pharmacogenomic approach used in this study may provide the basis for the use of molecular markers in the rational design of new clinical treatment paradigms.

Acknowledgments

We thank Jennifer Trevor, Kim Hoyle, and Suzanne Randall for technical assistance. We also thank Dr. Gretchen Cloud and Dr. Mark Carpenter for their aid with statistical analyses.

References

1. Galanis, E., and Buckner, J. C. Chemotherapy of brain tumors. Curr. Opin. Neurol., *13*: 619–625, 2000.

2. Macarthur, D. C., and Buxton, N. The management of brain tumours. J. R. Coll. Surg. Edinb., *46*: 341–348, 2001.

3. Prados, M. D., and Levin, V. Biology and treatment of malignant glioma. Semin. Oncol., *27*: 1–10, 2000.

4. Hildebrand, J., Sahmoud, T., Mignolet, F., Brucher, J. M., and Afra, D. Adjuvant therapy with dibromodulcitol and BCNU increases survival of adults with malignant gliomas. EORTC Brain Tumor Group. Neurology, *44*: 1479–1483, 1994.

5. Brem, H., Piantadosi, S., Burger, P. C., Walker, M., Selker, R., Vick, N. A., Black, K., Sisti, M., Brem, S., Mohr, G., *et al.* Placebo-controlled trial of safety and efficacy of intraoperative controlled delivery by biodegradable polymers of chemotherapy for recurrent gliomas. The Polymer-brain Tumor Treatment Group. Lancet, *345*: 1008–1012, 1995.

6. Subach, B. R., Witham, T. F., Kondziolka, D., Lunsford, L. D., Bozik, M., and Schiff, D. Morbidity and survival after 1,3-bis(2-chloroethyl)-1-nitrosourea wafer implantation for recurrent glioblastoma: a retrospective case-matched cohort series. Neurosurgery (Baltimore), *45*: 17–22; discussion 22–13, 1999.

7. Wang, M. L., Yung, W. K., Royce, M. E., Schomer, D. F., and Theriault, R. L. Capecitabine for 5-fluorouracil-resistant brain metastases from breast cancer. Am. J. Clin. Oncol., *24*: 421–424, 2001.

8. Bajetta, E., Carnaghi, C., Somma, L., and Stampino, C. G. A pilot safety study of capecitabine, a new oral fluoropyrimidine, in patients with advanced neoplastic disease. Tumori, *82:* 450–452, 1996.

9. Budman, D. R., Meropol, N. J., Reigner, B., Creaven, P. J., Lichtman, S. M., Berghorn, E., Behr, J., Gordon, R. J., Osterwalder, B., and Griffin, T. Preliminary studies of a novel oral fluoropyrimidine carbamate: capecitabine. J. Clin. Oncol., *16:* 1795–1802, 1998.

10. Ishikawa, T., Fukase, Y., Yamamoto, T., Sekiguchi, F., and Ishitsuka, H. Antitumor activities of a novel fluoropyrimidine, N4-pentyloxycarbonyl-5′-deoxy-5-fluorocytidine (capecitabine). Biol. Pharm. Bull., *21:* 713–717, 1998.

11. Heggie, G. D., Sommadossi, J. P., Cross, D. S., Huster, W. J., and Diasio, R. B. Clinical pharmacokinetics of 5-fluorouracil and its metabolites in plasma, urine, and bile. Cancer Res., *47:* 2203–2206, 1987.

12. Diasio, R. B., Beavers, T. L., and Carpenter, J. T. Familial deficiency of dihydropyrimidine dehydrogenase. Biochemical basis for familial pyrimidinemia and severe 5-fluorouracil-induced toxicity. J. Clin. Investig., *81:* 47–51, 1988.

13. Ishikawa, T., Sekiguchi, F., Fukase, Y., Sawada, N., and Ishitsuka, H. Positive correlation between the efficacy of capecitabine and doxifluridine and the ratio of thymidine phosphorylase to dihydropyrimidine dehydrogenase activities in tumors in human cancer xenografts. Cancer Res., *58:* 685–690, 1998.

14. Tsukamoto, Y., Kato, Y., Ura, M., Horii, I., Ishitsuka, H., Kusuhara, H., and Sugiyama, Y. A physiologically based pharmacokinetic analysis of capecitabine, a triple prodrug of 5-FU, in humans: the mechanism for tumor-selective accumulation of 5-FU. Pharm. Res., *18:* 1190–1202, 2001.

15. Schuller, J., Cassidy, J., Dumont, E., Roos, B., Durston, S., Banken, L., Utoh, M., Mori, K., Weidekamm, E., and Reigner, B. Preferential activation of capecitabine in tumor following oral administration to colorectal cancer patients. Cancer Chemother. Pharmacol., *45:* 291–297, 2000.

16. Nishimura, G., Terada, I., Kobayashi, T., Ninomiya, I., Kitagawa, H., Fushida, S., Fujimura, T., Kayahara, M., Shimizu, K., Ohta, T., and Miwa, K. Thymidine phosphorylase and dihydropyrimidine dehydrogenase levels in primary colorectal cancer show a relationship to clinical effects of 5′-deoxy-5-fluorouridine as adjuvant chemotherapy. Oncol. Rep., *9:* 479–482, 2002.

17. Eda, H., Fujimoto, K., Watanabe, S., Ura, M., Hino, A., Tanaka, Y., Wada, K., and Ishitsuka, H. Cytokines induce thymidine phosphorylase expression in tumor cells and make them more susceptible to 5′-deoxy-5-fluorouridine. Cancer Chemother. Pharmacol., *32:* 333–338, 1993.

18. Sawada, N., Ishikawa, T., Fukase, Y., Nishida, M., Yoshikubo, T., and Ishitsuka, H. Induction of thymidine phosphorylase activity and enhancement of capecitabine efficacy by taxol/taxotere in human cancer xenografts. Clin. Cancer Res., *4:* 1013–1019, 1998.

19. Endo, M., Shinbori, N., Fukase, Y., Sawada, N., Ishikawa, T., Ishitsuka, H., and Tanaka, Y. Induction of thymidine phosphorylase expression and enhancement of efficacy of capecitabine or 5′-deoxy-5-fluorouridine by cyclophosphamide in mammary tumor models. Int. J. Cancer, *83:* 127–134, 1999.

20. Sawada, N., Ishikawa, T., Sekiguchi, F., Tanaka, Y., and Ishitsuka, H. X-ray irradiation induces thymidine phosphorylase and enhances the efficacy of capecitabine (Xeloda) in human cancer xenografts. Clin. Cancer Res., *5:* 2948–2953, 1999.

21. Blanquicett, C., Johnson, M., Heslin, M., and Diasio, R. B. Housekeeping gene (HKG) variability in normal and carcinomatous colorectal and liver tissues; applications in pharmacogenomic gene expression studies. Anal. Biochem., *303:* 209–214, 2002.

22. Johnson, M. R., Wang, K., Smith, J. B., Heslin, M. J., and Diasio, R. B. Quantitation of dihydropyrimidine dehydrogenase expression by real-time reverse transcription polymerase chain reaction. Anal. Biochem., *278:* 175–184, 2000.

23. Andratschke, N., Grosu, A. L., Molls, M., and Nieder, C. Perspectives in the treatment of malignant gliomas in adults. Anticancer Res., *21:* 3541–3550, 2001.

24. Diasio, R. B., and Johnson, M. R. The role of pharmacogenetics and pharmacogenomics in cancer chemotherapy with 5-fluorouracil. Pharmacology (Basel), *61:* 199–203, 2000.

25. Salonga, D., Danenberg, K. D., Johnson, M., Metzger, R., Groshen, S., Tsao-Wei, D. D., Lenz, H. J., Leichman, C. G., Leichman, L., Diasio, R. B., and Danenberg, P. V. Colorectal tumors responding to 5-fluorouracil have low gene expression levels of dihydropyrimidine dehydrogenase, thymidylate synthase, and thymidine phosphorylase. Clin. Cancer Res., *6:* 1322–1327, 2000.

26. Johnson, M. R., Hsgeboutros, A., Wang, K., High, L., Smith, J. B., and Diasio, R. B. Life-threatening toxicity in a dihydropyrimidine dehydrogenase-deficient patient after treatment with topical 5-fluorouracil. Clin. Cancer Res., *5:* 2006–2011, 1999.

27. Mori, K., Hasegawa, M., Nishida, M., Toma, H., Fukuda, M., Kubota, T., Nagasue, N., Yamana, H., Hirakawa, Y. S. C. K., Ikeda, T., Takasaki, K., Oka, M., Kameyama, M., Tol, M., Fujii, H., Kitamura, M., Murai, M., Sasaki, H., Ozono, S., Makuuchi, H., Shimada, Y., Onishi, Y., Aoyagi, S., Mizutani, K., Ogawa, M., Nakao, A., Kinoshita, H., Tono, T., Imamoto, H., Nakashima, Y., and Manabe, T. Expression levels of thymidine phosphorylase and dihydropyrimidine dehydrogenase in various human tumor tissues. Int. J. Oncol., *17:* 33–38, 2000.

28. Wild-Bode, C., Weller, M., Rimmer, A., Dichgans, J., and Wick, W. Sublethal irradiation promotes migration and invasiveness of glioma cells: implications for radiotherapy of human glioblastoma. Cancer Res., *61:* 2744–2750, 2001.

29. Goto, H., Kohno, K., Sone, S., Akiyama, S., Kuwano, M., and Ono, M. Interferon γ-dependent induction of thymidine phosphorylase/platelet-derived endothelial growth factor through gamma-activated sequence-like element in human macrophages. Cancer Res., *61:* 469–473, 2001.

30. Knupfer, M. M., Poppenborg, H., Van Gool, S., Domula, M., and Wolff, J. E. Interferon-γ inhibits proliferation and adhesion of T98G human malignant glioma cells *in vitro*. Klin. Padiatr., *209:* 271–274, 1997.

31. Dadle, B., Schartner, J., Vorpahl, J., and Preston, K. Interferon-γ induces apoptosis and augments the expression of Fas and Fas ligand by microglia *in vitro*. Exp. Neurol., *162:* 290–296, 2000.

32. Mizutani, N., Fujikura, Y., Wang, Y. H., Tamechika, M., Tokuda, N., Sawada, T., and Fukumoto, T. Inflammatory and anti-inflammatory cytokines regulate the recovery from sublethal X irradiation in rat thymus. Radiat. Res., *157:* 281–289, 2002.

33. Fujieda, S., Sunaga, H., Tsuzuki, H., Fan, G. K., and Saito, H. IL-10 expression is associated with the expression of platelet-derived endothelial growth factor and prognosis in oral and oropharyngeal carcinoma. Cancer Lett., *136:* 1–9, 1999.

34. Denys, A., Udalova, I. A., Smith, C., Williams, L. M., Ciesielski, C. J., Campbells, A. J., Andrews, C., Kwiatkowski, D., and Foxwell, B. M. Evidence for a dual mechanism for IL-10 suppression of TNF-α production that does not involve inhibition of p38 mitogen-activated protein kinase of NF-κB in primary human macrophages. J. Immunol., *168:* 4837–4845, 2002.

35. Filkington, G. J. The paradox of neoplastic glial cell invasion of the brain and apparent metastatic failure. Anticancer Res., *17:* 4103–4105, 1997.

36. Wilke, H. Future treatment options with Capecitabine in solid tumours. Eur. J. Cancer, *38:* 21–25, 2002.